USGS
science for a changing world

Three-Dimensional Geologic Mapping of the Cenozoic Basin Fill, Amargosa Desert Basin, Nevada and California

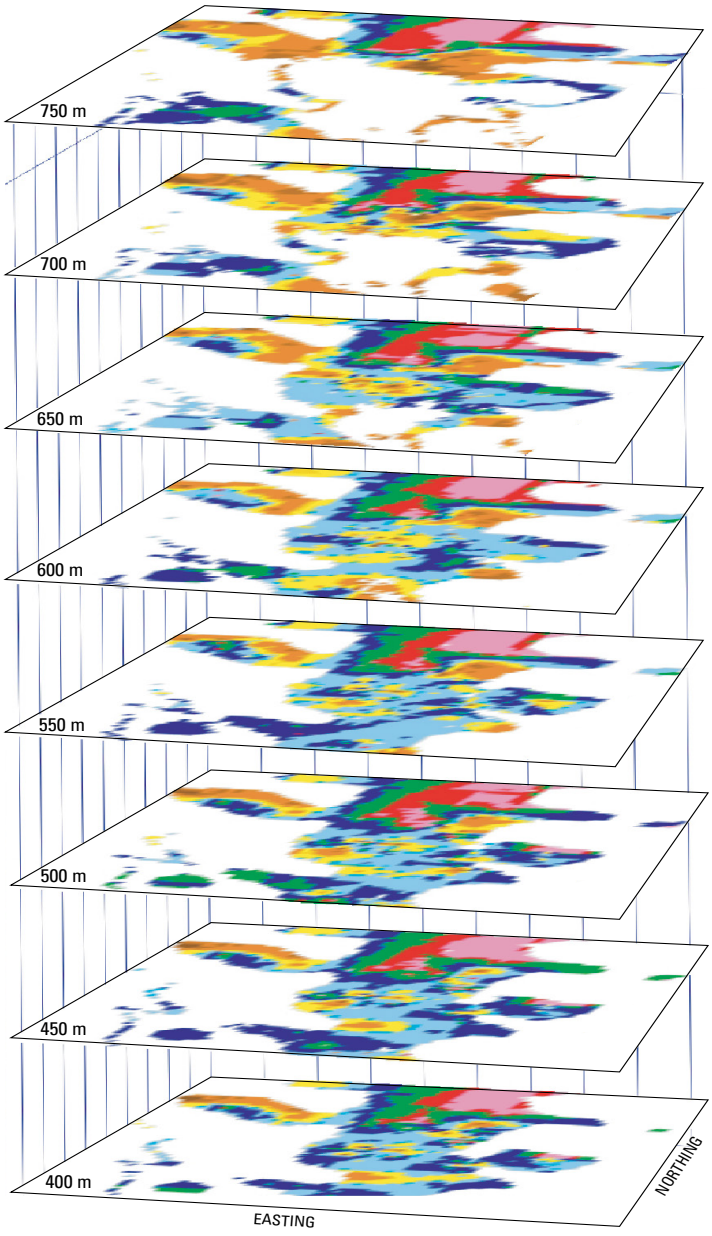

Scientific Investigations Report 2014–5003

U.S. Department of the Interior
U.S. Geological Survey

COVER. Perspective views of horizontal sections cut through the 3D interpreted–facies model of the Amargosa Desert. See figure 9 this report.

Three-Dimensional Geologic Mapping of the Cenozoic Basin Fill, Amargosa Desert Basin, Nevada and California

By Emily M. Taylor and Donald S. Sweetkind

Scientific Investigations Report 2014–5003

U.S. Department of the Interior
U.S. Geological Survey

U.S. Department of the Interior
SALLY JEWELL, Secretary

U.S. Geological Survey
Suzette Kimball, Acting Director

U.S. Geological Survey, Reston, Virginia: 2014

Suggested citation:
Taylor, E.M., and Sweetkind, D.S., 2014, Three-dimensional geologic mapping of the Cenozoic basin fill, Amargosa Desert basin, Nevada and California: U.S. Geological Survey Scientific Investigations Report 2014–5003, 40 p., 2 appendixes, *http://dx.doi.org/10.3133/sir20145003*.

ISSN 2328-0328 (online)

Contents

Figures

Tables

Conversion Factors

Inch/Pound to SI

Multiply	By	To obtain
	Length	
inch (in.)	2.54	centimeter (cm)
inch (in.)	25.4	millimeter (mm)
foot (ft)	0.3048	meter (m)
mile (mi)	1.609	kilometer (km)
yard (yd)	0.9144	meter (m)

Three-Dimensional Geologic Mapping of the Cenozoic Basin Fill, Amargosa Desert Basin, Nevada and California

By Emily M. Taylor and Donald S. Sweetkind

Abstract

Understanding the subsurface geologic framework of the Cenozoic basin fill that underlies the Amargosa Desert in southern Nevada and southeastern California has been improved by using borehole data to construct three-dimensional lithologic and interpreted facies models. Lithologic data from 210 boreholes from a 20-kilometer (km) by 90-km area were reduced to a limited suite of descriptors based on geologic knowledge of the basin and distributed in three-dimensional space using interpolation methods. The resulting lithologic model of the Amargosa Desert basin portrays a complex system of interfingered coarse- to fine-grained alluvium, playa and palustrine deposits, eolian sands, and interbedded volcanic units. Lithologic units could not be represented in the model as a stacked stratigraphic sequence due to the complex interfingering of lithologic units and the absence of available time-stratigraphic markers. Instead, lithologic units were grouped into interpreted genetic classes, such as playa or alluvial fan, to create a three-dimensional model of the interpreted facies data. Three-dimensional facies models computed from these data portray the alluvial infilling of a tectonically formed basin with intermittent internal drainage and localized regional groundwater discharge. The lithologic and interpreted facies models compare favorably to resistivity, aeromagnetic, and geologic map data, lending confidence to the interpretation.

Introduction

The Amargosa Desert basin is an intermontane basin that lies beneath the Amargosa Desert in southern Nevada and southeastern California (Stonestrom and others, 2007) (fig. 1*A*). The basin comprises a complex assemblage of Tertiary sediments and Quaternary deposits deposited in a trough to the northeast of the Funeral Mountains and to the southwest uplifted pre-Tertiary rocks exposed at Bare Mountain and in the Specter Range (fig. 1*B*).

The basin is a critical part of the regional groundwater flow system that includes Death Valley, California, and the Nevada National Security Site (formerly the Nevada Test Site) (Winograd and Thordarson, 1975). Groundwater of the Amargosa Desert basin serves as the sole water source for a number of agricultural, commercial, and residential users; supports a thriving agricultural community; serves as habitat for the endangered desert pupfish at regional springs in Ash Meadows (Winograd and Thordarson, 1975; Dudley and Larson, 1976); and some of the water ultimately discharges at springs in Death Valley (Hunt and others, 1966; Steinkampf and Werrell, 2001; Belcher and others, 2009). The Cenozoic rocks and deposits of the Amargosa Desert basin have great lithologic diversity including coarse- and fine-grained alluvial fill; groundwater discharge, playa, and eolian deposits; reworked tuffs; and tuffaceous sedimentary rocks and volcanic rocks that span an age range from Oligocene to Pliocene (Denny and Drewes, 1965; Naff, 1973; Oatfield and Czarnecki, 1989, 1991; Sweetkind and others, 2001). These rocks and deposits also show large variations in hydrologic behavior (Fenelon and Moreo, 2002). However, the configuration and continuity of basin-fill units that serve as aquifers within the Amargosa Desert basin is poorly known, leading to difficulties in estimating the available exploitable groundwater resource, a lack of ability to understand and respond to water-level declines created by groundwater withdrawals, and a lack of ability to evaluate issues of groundwater quantity and quality. Better prediction of the effects of groundwater development on regional springs and associated biota and habitats and the susceptibility of groundwater resources to pumping will result from improved understanding of the hydrogeologic system.

The local and regional importance of the groundwater aquifers within the Amargosa Desert basin, combined with the proximity to the Nevada National Security Site and the previously proposed high-level nuclear waste repository at Yucca Mountain, Nevada, have given rise to a number of topical studies that provided critical data and interpretations of the subsurface geology in this region. However, none of these studies attempted an integrated, three-dimensional (3D) portrayal of the basin-filling units. Detailed geologic maps that emphasized surficial geologic units are available for parts of the Amargosa Desert (Denny and Drewes, 1965; Swadley, 1983; Swadley and Carr, 1987); more generalized regional geologic maps also exist (Workman and others, 2002). Topical

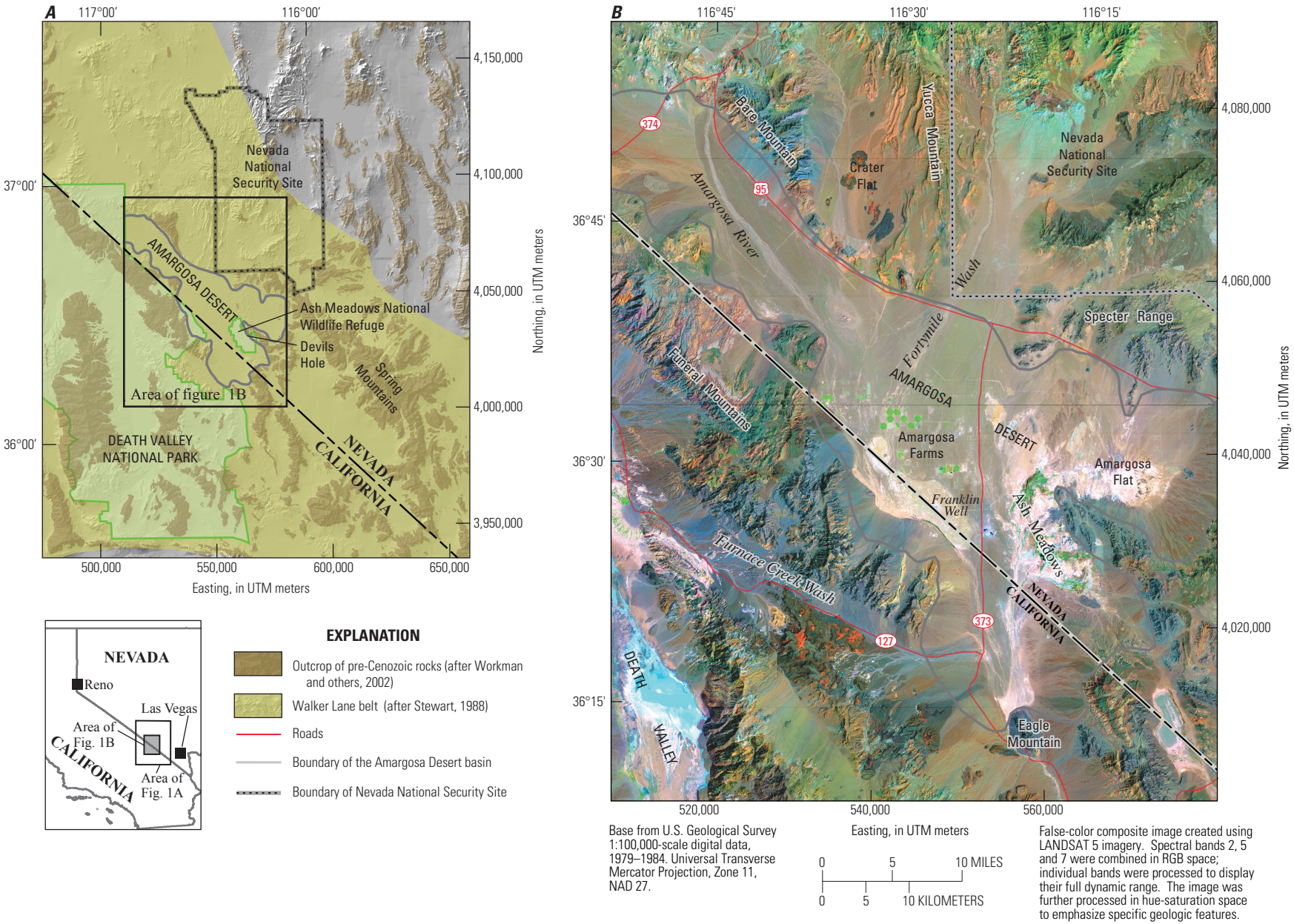

Figure 1. Location of the Amargosa Desert basin. *A,* Location relative to Death Valley and pre-Cenozoic rocks surrounding the basin. *B,* Location of physiographic features within the basin boundary.

studies of the Miocene and Pliocene basin-fill sedimentary rocks and interbedded volcanic rocks have provided insights into the timing and style of basin opening and filling (Çemen, 1999; Fridrich, 1999; Sweetkind and others, 2001; Fridrich and Thompson, 2011). Geophysical studies have used gravity data to elucidate the shape and depth of the basin (Blakely and others, 1998, 1999; Blakely and Ponce, 2001). Aeromagnetic data have defined the spatial extent and general shapes of the major magnetic bodies within the basin fill, which are predominantly volcanic rocks (Blakely and others, 2000). Ground-magnetic surveys have helped to define the size, shape, and estimated depth of these magnetic sources (Langenheim, 1995; O'Leary and others, 2002; Blakely and others, 2005).

This report includes the following elements:

1. A description of the construction of preliminary 3D digital models of lithology and depositional facies using a subset of the well data and of the construction of 3D resistivity models from published resistivity data collected along several profiles in the basin, and

2. A description of the results of these models along several lines of section in several places in the basin, pointing out geologically and hydrologically significant aspects of the data and models.

The following appendixes are not in the body of the report but are two separate files located on this publication's Web index page *http://pubs.usgs.gov/sir2014/5003*:

Appendix 1–A data appendix that contains locational and lithologic descriptors for 435 boreholes drilled in the Amargosa Desert basin, of which 210 were used to model the subsurface, and

Appendix 2–A data appendix that contains locational descriptors and resistivity soundings in the Amargosa Desert basin;

The 3D modeling discussed in this report was the product of preliminary work in the basin conducted in 2002–2004 as part of a geologic investigation of the Amargosa basin fill. Work in the basin has continued in subsequent years, resulting in the compilation of a number of drill holes not used in the initial data compilation and modeling. Because all of the well data were treated in the same way, all of the well data compiled to date are included in appendix 1, although only a subset of those data were used to construct the 3D models. Those wells that were used in the preliminary 3D digital models are distinguished in appendix 1 from those wells that are reported only in the appendix.

This report documents the development of 3D digital models that characterize the basin-filling rocks and deposits beneath the Amargosa Desert in southern Nevada and southeastern California. Lithologic data from 210 boreholes in the basin are compiled to describe lithologic variations and distributions of grain size within the basin-fill rocks and deposits. Lithologic data are interpreted in terms of stratigraphic facies based upon surface mapping data, knowledge of facies-based depositional processes in continental depositional settings, regional geologic history, basin aggradation rates, drainage evolution, fault activity, and structural history. 3D digital models of the sedimentary-facies architecture of the consolidated, mostly Tertiary units in the basin and younger unconsolidated deposits are based on the interpreted borehole data.

The preliminary 3D models are mathematically relatively crude in that they are deterministic and do not account for spatial structure in the subsurface data. Yet these models are a way to visualize, in three dimensions, the lithologic and facies data that have been derived from diverse driller's descriptions. These simplistic models offer a starting point to interpreting the subsurface lithologic variability of this region and highlight in three dimensions the geologic data included in the compilation of well data.

Geologic and Tectonic Setting

Consolidated rocks that fill the deeper parts of the Amargosa Desert basin range in age from Oligocene to Pliocene; younger basalt flows are also present in the overlying unconsolidated Quaternary section. Consolidated Cenozoic rocks include coarse- to fine-grained sedimentary rocks of variable sorting and bedding characteristics, predominantly fine-grained groundwater discharge and playa deposits, tuffaceous sedimentary rocks and reworked tuffs, and volcanic rocks that include welded and nonwelded ash-flow tuffs, basalts, and tephra (fig. 2A). Cenozoic sedimentary rocks were deposited before, during, and after regional extension and volcanism (Çemen and others, 1999; Snow and Lux, 1999; Sweetkind and others, 2001). In general, Miocene and older sedimentary rocks are tilted and faulted and likely segmented within the basin by numerous faults. Miocene and Pliocene volcanic rocks of the southwestern Nevada volcanic field (Sawyer and others, 1994) and the central Death Valley volcanic field (Wright and others, 1991) are exposed in highlands to the north and southwest, respectively, of the Amargosa Desert basin and are associated with pronounced high-amplitude, short-wavelength magnetic anomalies (Blakely and others, 2000) (fig. 2*B*). The general absence of strong magnetic anomalies in the vicinity of the Amargosa Desert implies that strongly magnetic volcanic rocks from either field are thin or deeply buried (Blakely and others, 2000). Deep boreholes drilled within or at the margins of the two volcanic fields penetrate volcanic rocks or interbedded sedimentary and volcanic rocks, whereas shallow water wells drilled in the center of the Amargosa Desert basin typically intercept only sedimentary rocks (figs. 2*A* and 2*B*). Volcanic rocks are interpreted to be present in the subsurface in the northwestern arm of the Amargosa Desert basin based on aeromagnetic data (fig. 2*B*), borehole intercepts, and isolated outcrops of Miocene Timber Mountain Group tuffs. Locally present within the basin fill are basaltic volcanic centers, as indicated by the presence of circular magnetic anomalies (Langenheim, 1995; O'Leary and others, 2002) and corroborated by limited borehole data.

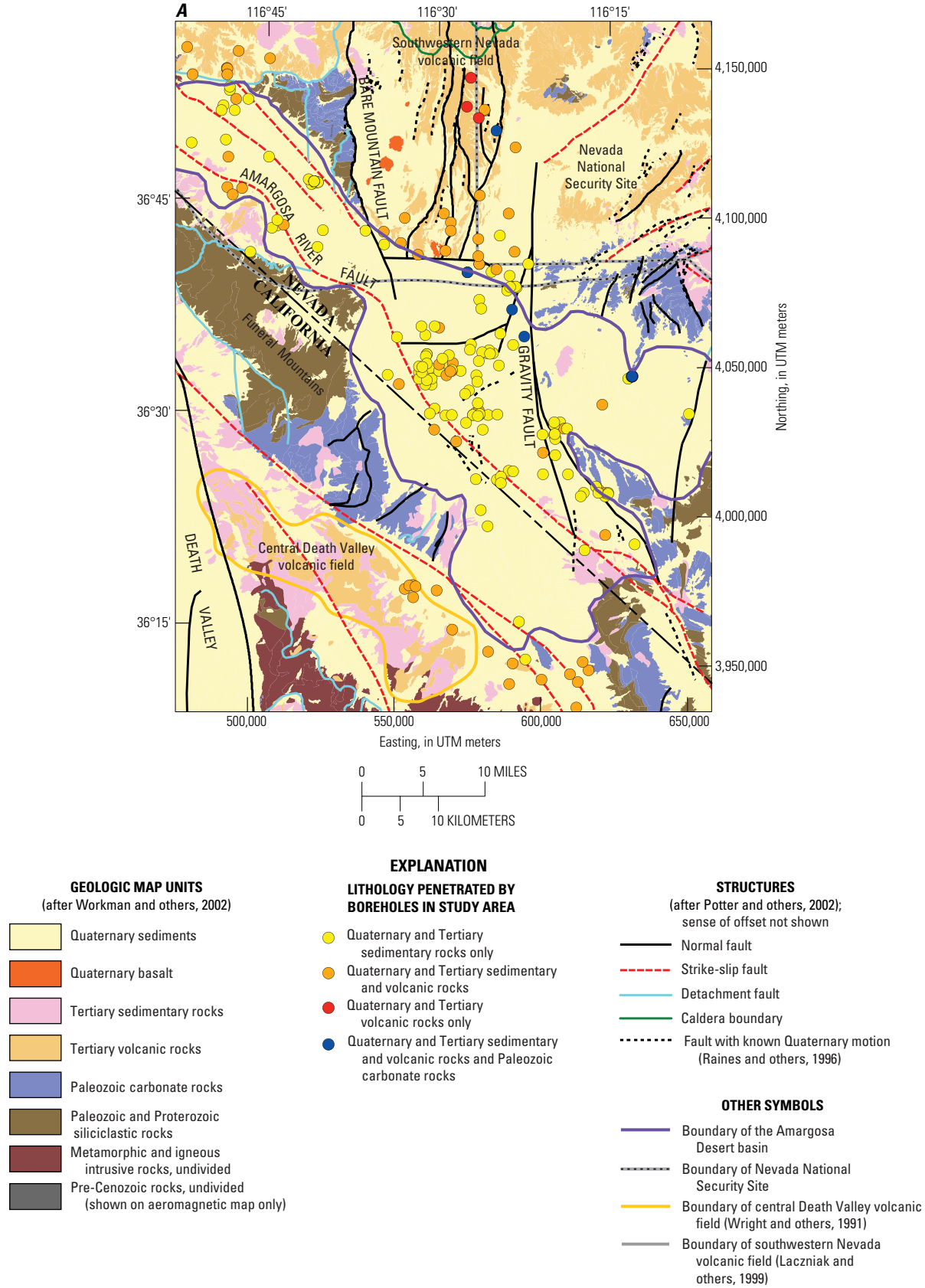

Figure 2. Maps of the Amargosa Desert basin showing lithology present in boreholes with: *A,* Geologic map units and structures and *B,* Aeromagnetic data and structure.

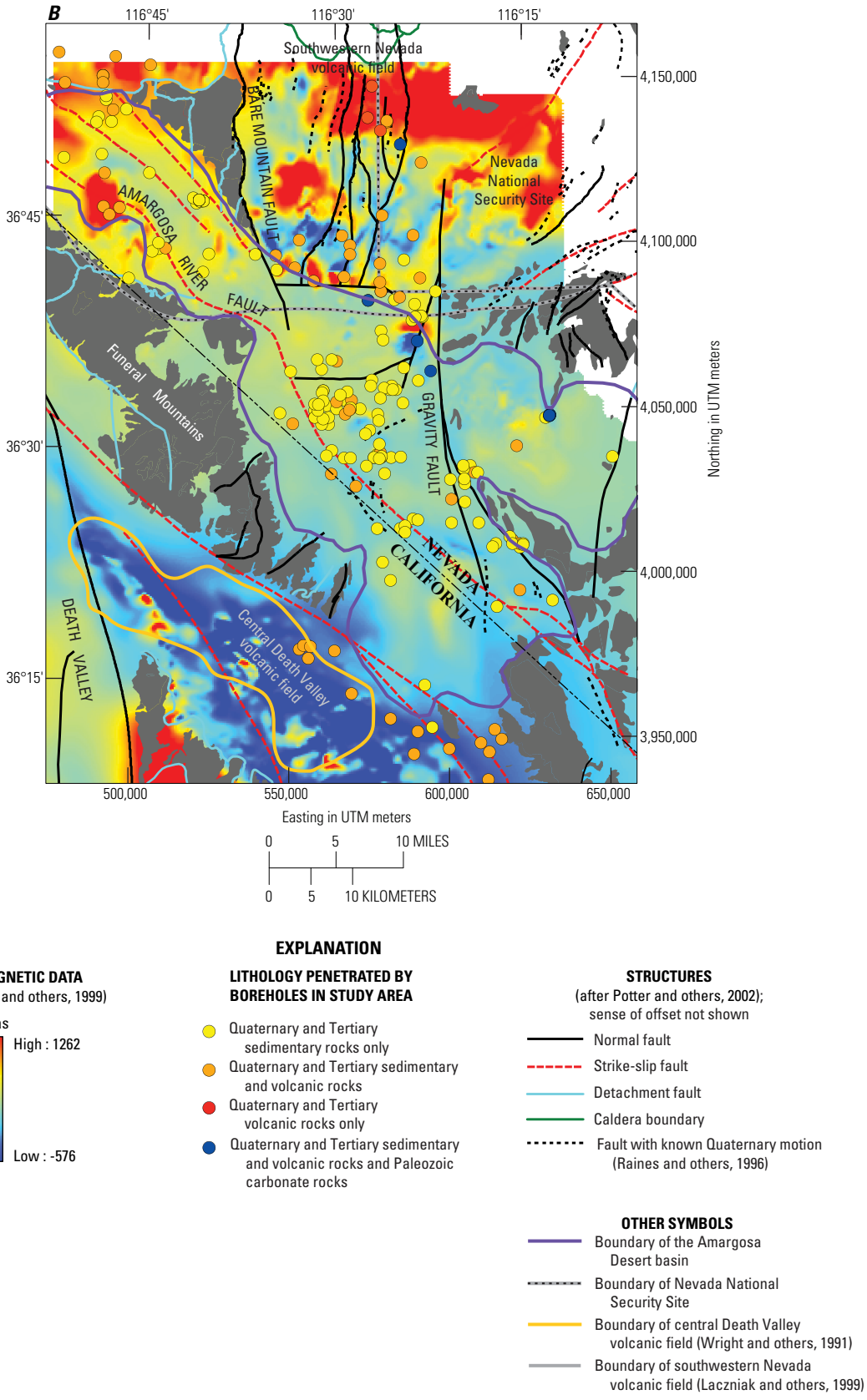

Figure 2—Continued. Maps of the Amargosa Desert basin showing lithology present in boreholes with: *A,* Geologic map units and structures and *B,* Aeromagnetic data and structure.

Unconsolidated Quaternary deposits within the basin include coarse- and fine-grained alluvial fan and stream-channel deposits; spring-discharge deposits; and eolian deposits, as both widespread sand sheets and more localized dunes. In general, coarse alluvial deposits occur adjacent to mountain fronts and these deposits grade basinward to finer-grained material. The major drainages of the Amargosa River and Fortymile Wash (fig. 1*B*) are incised into older, partly consolidated basin fill that is exposed in the walls of the modern washes. The confluence of these two drainages occurs in the center of the basin. In the Amargosa Desert basin, alluvial terraces less than 2 meters above the active channel are preserved adjacent to the Amargosa River and Fortymile Wash. Similar aged terraces as those in the basin are tens of meters above the active channel in the narrow canyons upstream of the basin. Light-colored, fine-grained spring discharge deposits are widespread in the southern part of the basin, south of Amargosa Farms and at Ash Meadows (fig. 1*B*). These deposits are fine-grained sands and silts that accumulated in soggy groundwater discharge or palustrine environments. The broad distribution of these deposits in the southern part of the basin preserves the record of more broadly distributed discharge that may reflect an environment much wetter than the modern climate (Hay and others, 1986); modern discharge is restricted to a considerably smaller area in the vicinity of Ash Meadows (Winograd and Thordarson, 1975).

The Amargosa Desert basin lies within the Walker Lane belt (Stewart, 1988) and is characterized by a mix of strike-slip and normal faults that reflect the varying influence of extensional and strike-slip deformation. Interpretations of gravity and magnetic data (Blakely and others, 1999) suggest that the Stewart Valley–Pahrump fault zone extends northwestward across the Amargosa Desert roughly parallel to the Nevada–California border, where it has been named the Amargosa River fault (figs. 2*A* and 2*B*) (Workman and others, 2002). Gravity data (Blakely and others, 1998, 1999) portray a structurally complex pre-Cenozoic surface adjacent to the Amargosa River fault consisting of steep-sided local depressions and ridges that must be fault bounded and probably represent local contraction and extension within the overall strike-slip environment (Stewart, 1988; Wright, 1989). The deepest part of the Amargosa Desert basin is bounded on the west by the Bare Mountain normal fault and on the east by the Gravity fault (figs. 2*A* and 2*B*) (Blakely and others, 1998, 1999; Blakely and Ponce, 2001).

Although faults were not explicitly included as part of the 3D modeling discussed in this report, they are used in interpreting the general lithologic patterns in the resulting models. Juxtaposition of contrasting geologic units along Neogene normal faults has been instrumental in localizing significant groundwater discharge in the Amargosa Desert basin. For example, a southeastern splay of the Gravity fault localizes a line of large discharge springs at Ash Meadows (fig. 1*B*) (Winograd and Thordarson, 1975). Regional northeast-to-southwest groundwater flow within Paleozoic carbonate rocks is likely diverted to the surface where these rocks are juxtaposed against the low-permeability basin-fill materials across the Gravity fault (Winograd and Thordarson, 1975). Discontinuous local aquifers, including coarse siliciclastic material and travertine deposits within the basin fill, provide flow paths to discharge sites at some distance from the Gravity fault in this area (Dudley and Larsen, 1976). More diffuse discharge is present in the vicinity of Franklin Well and at Amargosa Flat (fig. 1*B*) (Laczniak and others, 1999).

Sources of Subsurface Data

Subsurface data are derived from boreholes (table 1) drilled in the Amargosa Desert basin for a variety of reasons, including mineral exploration (U.S. Borax and Bond Gold, table 1), oil and gas exploration (Felderhoff Federal, table 1), agricultural and domestic water wells (Amargosa Farms, table 1), site characterization associated with the U.S. Department of Energy's Yucca Mountain program (U.S. Geological Survey (USGS) Yucca Mountain project, table 1), the Nye County Early Warning Drilling Program to the south of Yucca Mountain (Nye County–EWDP, table 1), and site-specific studies such as the USGS tracer study, and monitoring at the US Ecology waste site (US Ecology, table 1). All borehole data were used from the above-mentioned data sources with the exception of water-well data from the Amargosa Farms where a total of 99 holes were selected from many hundreds of available boreholes. The 99 selected boreholes represented those that could be most accurately located, had a total depth greater than 100 meters (m), contained the greatest amount of detail in the driller's lithologic descriptions, and provided a roughly regularly spaced distribution of boreholes where the data were not clustered.

The accuracy of the water-well borehole location is variable within these data. In some cases, boreholes could be located based on a street address; the most poorly located boreholes were plotted at the center of a quarter section. No attempt was made to locate water-well boreholes accurately through field checking, nor through comparison with aerial photographs. The remaining boreholes, drilled for exploration and monitoring, were located with a high degree of accuracy and checked with National Water Information System (NWIS) locations (USGS, 2001).

A total of 210 boreholes were selected to characterize the subsurface (table 1). Our database (appendix 1) also includes boreholes that were drilled after our lithology model was built and before publication. Most of the boreholes do not penetrate the entire Tertiary section, resulting in a bias towards data from the upper part of the section. Gravity models predict that the Cenozoic section is 1 to 2 km thick within the Amargosa Desert basin (Blakely and others, 1999), so most of the boreholes intersect only unconsolidated sediment and sedimentary rocks (131 holes). Most of the remaining boreholes intersect Cenozoic sedimentary and volcanic rocks (70 holes); only 9 boreholes penetrate the entire Cenozoic section and bottom

Table 1. Description of borehole data.

Data set	Reference	Total number of holes	Mean total depth, meters	Number of holes penetrating specific rock type		
				Sedimentary rocks only	Sedimentary and volcanic rocks	Sedimentary and volcanic rocks, and Paleozoic carbonate rocks
Amargosa Farms	State of Nevada, Department of Conservation and Natural Resources (data accessed 2007)	99	166	87	12	0
Amargosa percolation test	Stonestrom and others (2003)	9	130	8	1	0
Bond Gold	William Werrell, National Park Service, written commun., 1989	17	281	10	7	0
Felderhoff Federal	Carr and others (1995)	2	988	0	0	2
Nye County Early Warning Drilling Program (EWDP)	Nye County Nuclear Waste Repository Project Office (NWRPO); Rick Spengler, U.S. Geological Survey, written commun., 2002	22	430	4	17	1
U.S. Borax	John Rodgers, U.S. Borax, written commun., 1996	36	465	11	25	0
U.S. Department of Energy	State of Nevada, Department of Conservation and Natural Resources (data accessed 2007)	2	630	1	1	0
US Ecology	State of Nevada, Department of Conservation and Natural Resources (data accessed 2007); Taylor (2010)	9	121	9	0	0
U.S. Geological Survey Tracer Study	Johnston (1968)	7	213	1	1	5
U.S. Geological Survey Yucca Mountain Project	Spengler and others (1979); Bentley and others (1983); Byers and Warren (1983); Maldonado and Koether (1983); Craig and Johnson (1984); Lahoud and others (1984); Whitfield and others (1984);	7	302	0	6	1
	Total number of holes	210	---	131	70	9

in Paleozoic carbonate rocks (fig. 3; table 1). The mean total depth for all the boreholes is 297 m, although total depth varies greatly by dataset (fig. 3; table 1).

Vertical electric resistivity soundings were conducted at 136 locations in the Amargosa Desert (Greenhaus and Zablocki, 1982) and 29 locations in the vicinity of Yucca Mountain (Senterfit and others, 1982) to define basement structure and basin-fill characteristics. In each study, raw resistivity data were processed and fitted with a step-function curve that represented a horizontally layered model that best fit the resistivity soundings. The modeled data depicted discrete intervals of varying resistivity to depths down to about 2 km (Greenhaus and Zablocki, 1982; Senterfit and others, 1982) (appendix 2). Oatfield and Czarnecki (1989) used an average resistivity value at each sounding location to create a contoured resistivity map of the Amargosa Desert. The step-function model results from the vertical electric resistivity soundings from all 29 locations in the vicinity of Yucca Mountain (Senterfit and others, 1982) and 50 selected locations from the northern part of the Amargosa Desert were digitized from the paper records (appendix 2). The result was a vertical succession of data points having varying values of resistivity beneath each surface sounding location.

3D Display of Surface and Subsurface Data

Three-dimensional perspective views of the Amargosa Desert portray the physiography of the region, the surficial geology, the modeled depth to pre-Cenozoic rocks, a 3D portrayal of the borehole data used in this study, and the results of the 3D lithology model. These perspective views illustrate some of the input datasets used in the 3D modeling to better understand the geology buried at depth.

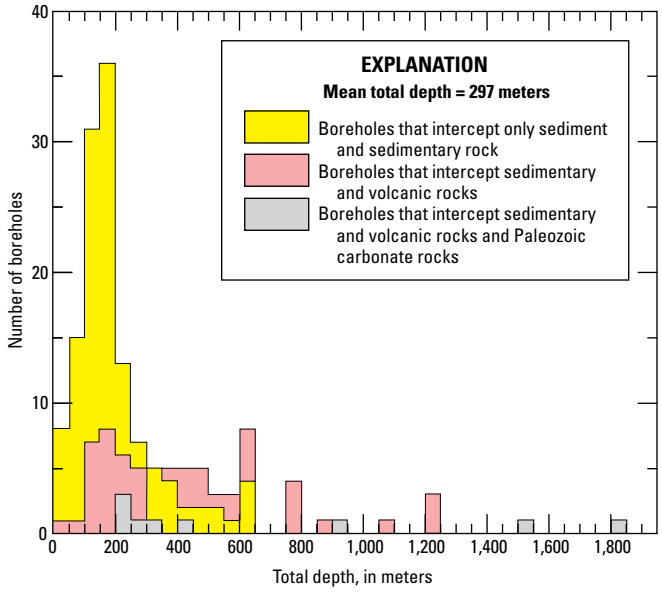

Figure 3. Frequency of drilling depths and lithologic units penetrated.

Physiography

A false-color composite Landsat 5 image was draped over a Digital Elevation Model (DEM) to emphasize the physiography of the Amargosa Desert (fig. 4). The view is from above and the southeast, looking northwest; a part of Death Valley is shown in the southwest corner of the view. On the image, bedrock exposures of Paleozoic carbonate rocks appear in shades of blue and green, such as in the Specter Range and at Bare Mountain; Proterozoic siliciclastic rocks appear in red-brown tones in the central Funeral Mountains. Bedrock exposures of rhyolitic volcanic rocks in the vicinity of Yucca Mountain appear in shades of tan and orange; Quaternary basalt flows in Crater Flat stand out as circular patches of black and orange. The colors of the basin-filling alluvial fans often reflect the lithology of their source areas. The confluence of the Amargosa River and Fortymile Wash occurs in the center of the basin. The light-colored deposits south of the confluence are fine-grained sands and silts that accumulated in groundwater discharge or palustrine environments. Playa and basin-axis deposits appear in white or light pink tones; the salt pan in Death Valley appears in bright blue. The Amargosa Desert is, in general, sparsely vegetated. Irrigated agricultural land in the Amargosa Farms area appears as bright green.

Modeled Top of Pre-Cenozoic Rocks and Borehole Data

The modeled elevation of the top of pre-Cenozoic rocks (fig. 5) is based on a computational inversion of gravity data (Blakely and others, 1999; Blakely and Ponce, 2001) that separates the gravitational effects of Cenozoic volcanic and sedimentary rocks from the denser pre-Cenozoic rocks in order to estimate the thickness of Cenozoic basin fill. Figure 5 portrays the modeled pre-Cenozoic surface as if the Cenozoic basin fill of the Amargosa Desert basin and surrounding regions had been removed. The elevation of the modeled pre-Cenozoic surface varies from about 1,400 to -2,900 m. The highest elevations correspond to outcrops of pre-Cenozoic rocks in the mountain ranges surrounding the Amargosa Desert basin; the lowest elevations correspond to deep basins and correspondingly thick accumulations of Cenozoic rocks. The deepest basins lie beneath Crater Flat and Yucca Mountain to the north of the Amargosa Desert, and beneath Death Valley to the west (fig. 5). Within the Amargosa Desert basin, the pre-Cenozoic rocks are deepest within a north-striking graben that is bounded on the west by uplifted pre-Cenozoic rocks at Bare Mountain and the Funeral Mountains, and on the east by the uplifted pre-Cenozoic rocks exposed in the Calico Hills, the Specter Range, and the Resting Spring Range (fig. 5). Gravity data show that the deep basin beneath Crater Flat and

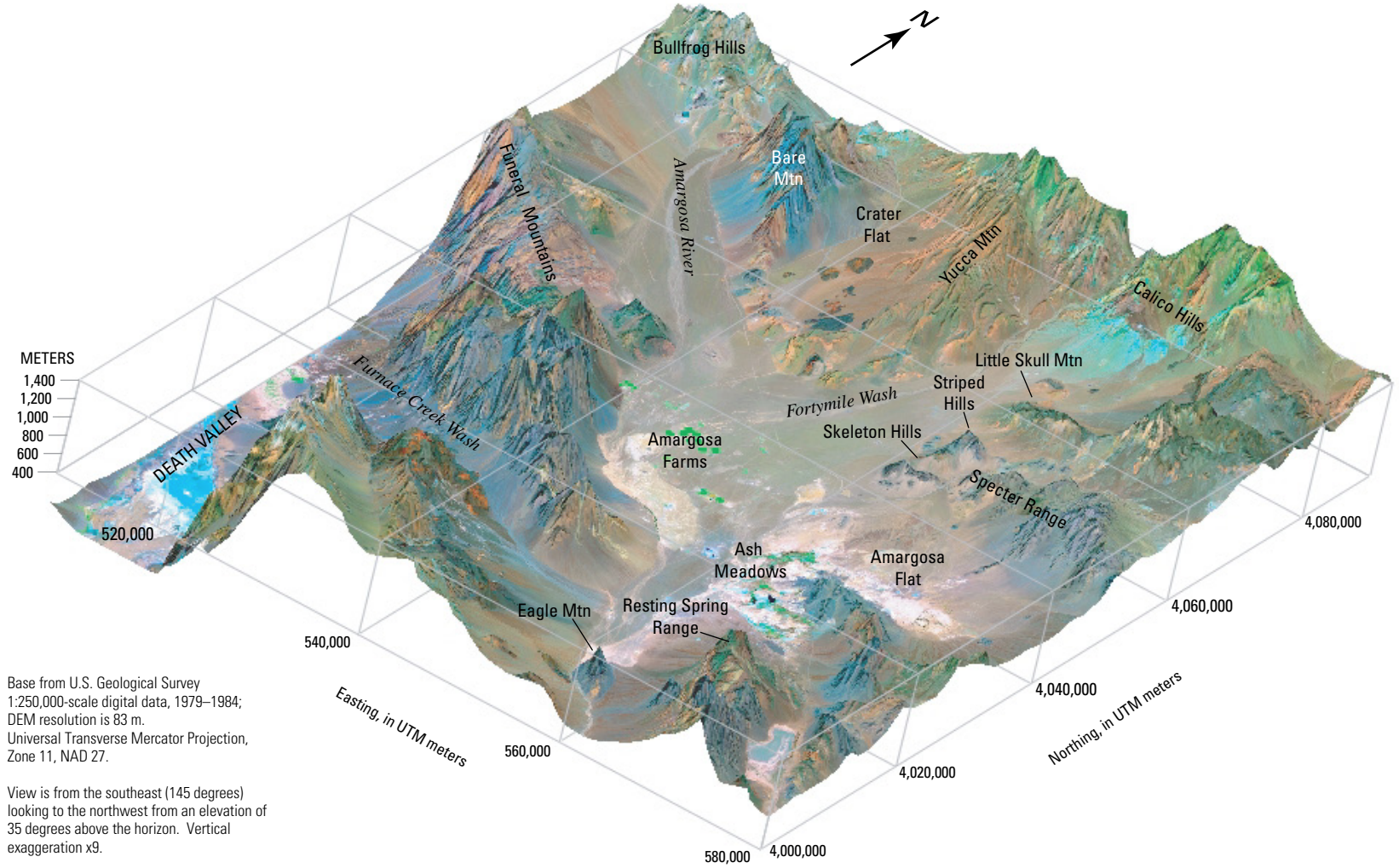

Base from U.S. Geological Survey
1:250,000-scale digital data, 1979–1984;
DEM resolution is 83 m.
Universal Transverse Mercator Projection,
Zone 11, NAD 27.

View is from the southeast (145 degrees) looking to the northwest from an elevation of 35 degrees above the horizon. Vertical exaggeration x9.

Figure 4. 3D perspective view showing false-color composite image of Amargosa Desert basin draped over a digital elevation model.

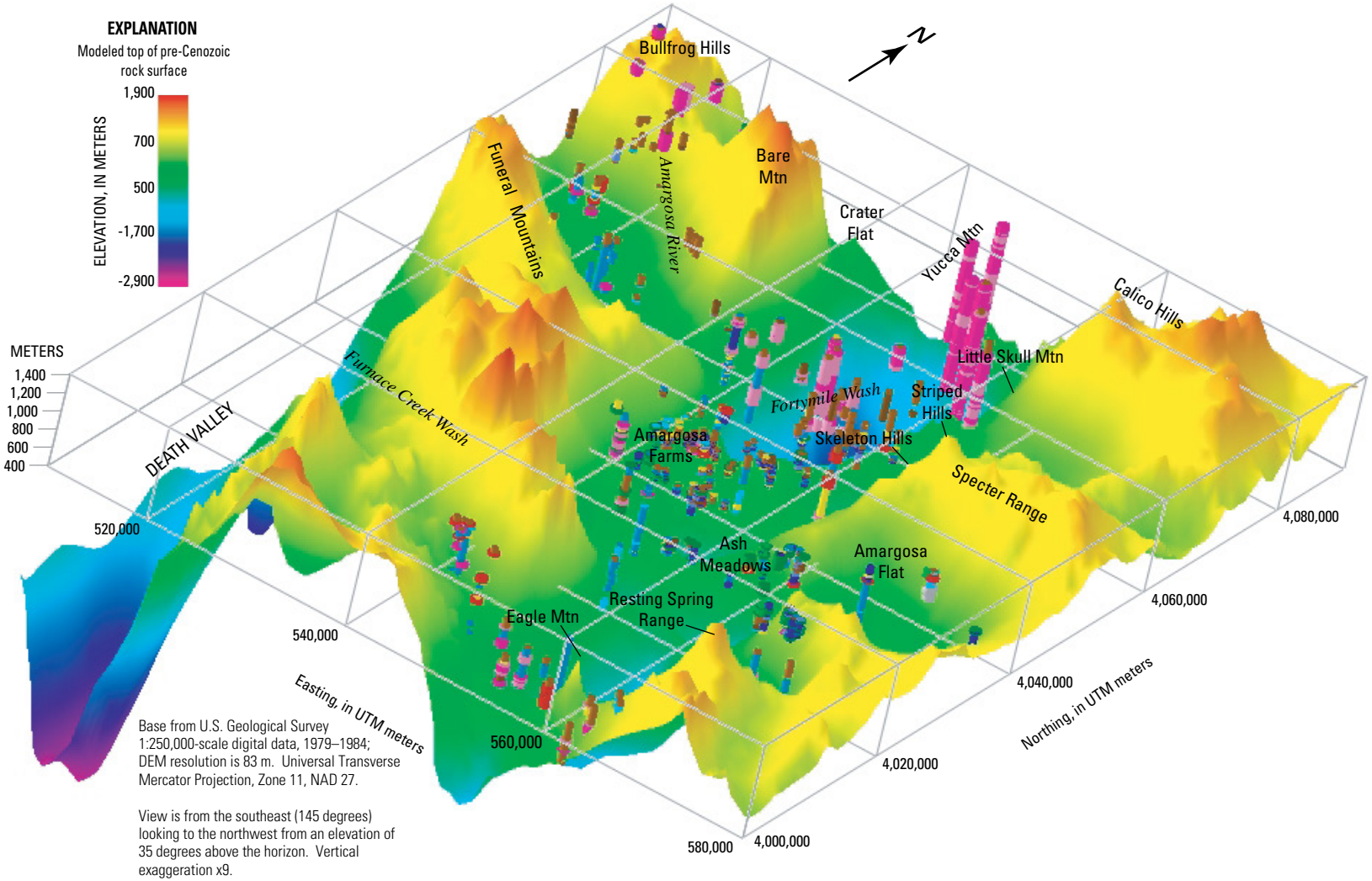

Figure 5. 3D perspective view showing modeled elevation of the top of pre-Cenozoic rocks and lithology intervals in boreholes. Cylinders represent the location and interval of boreholes that penetrated Cenozoic rocks; colors represent lithologic units intercepted downhole. Colors appear variable due to the effects of illumination from below and southwest. Boreholes are hung from their collar elevation at land surface. Land surface is transparent; as a result, the boreholes have the appearance of hanging in space.

Yucca Mountain is separated from smaller sub-basins beneath the southern part of the Amargosa Desert by a saddle of relatively higher pre-Cenozoic rocks just west of the Skeleton Hills (Blakely and others, 1998, 1999). Two oil exploration wells (Felderhoff Federal) were drilled on this saddle in the northern part of the Amargosa Desert and penetrated Paleozoic carbonate rocks (Carr and others, 1995).

Boreholes used in this study are shown with the modeled top of pre-Cenozoic rocks (Blakely and Ponce, 2001) in 3D perspective view (fig. 5). Boreholes are shown as cylinders that are colored according to the lithologic descriptors listed in table 2. Land surface is transparent in this view and the basin-fill rocks are "removed" to show the pre-Cenozoic surface, so boreholes appear to hang in space.

Surficial Geology

A geologic map of Cenozoic and pre-Cenozoic geologic units (modified from Workman and others, 2002) draped over the DEM emphasizes the present-day surficial geologic setting (fig. 6). All pre-Cenozoic rocks and Cenozoic volcanic rocks are shown as a single undivided unit (dark brown, fig. 6). Surficial geologic units mapped in the Amargosa Desert are characterized by coarse alluviation (dark yellow, fig. 6) in major channels, including the Amargosa River and Fortymile Wash, and adjacent to the mountain fronts. This coarse material grades to finer-grained deposits in the basin axis (light yellow, fig. 6). The major drainages of the Amargosa River and Fortymile Wash are incised into older, indurated alluvium that is exposed in the walls of the modern washes. Fine-grained deposits associated with groundwater discharge (light blue, fig. 6), are infrequently interfingered with coarse- to fine-grained alluvium.

3D Modeling Methods

Lithologic descriptions from the borehole data were interpreted to derive an internally consistent set of lithologic and depositional environment descriptors; interpretations were informed by surface mapping data. Data quality is variable; detailed lithologic descriptions were recorded in most of the datasets, with the exception of boreholes for domestic and (or) agricultural usage (Oatfield and Czarnecki, 1989). The original driller's lithologic descriptions were simplified to a limited number of standardized lithologic units (table 2). For example, "clay and sand," typical lithology of a playa deposit, could have been any of the following in the driller's original log—mudstone, sandy clay, sandy siltstone, and silty clay. "Sand and gravel" was simplified from driller's descriptions boulders and clay, boulders and sand, gravel and clay, and sandy gravel. Unit cementation was eliminated during this process of simplifying the lithology; for example, sandstone was described as the unit "sand," and conglomerate as the unit "sand, clay, and gravel." The descriptor "silt" was not used, because it is infrequently used, generally inaccurately, when describing sampled material. Units described as containing silt were given the lithologic descriptor "sand and clay."

Three-dimensional models were created from the borehole data using the RockWorks2004 software package (RockWare, 2004). The 3D-lithology solid model was created from the borehole data using a nearest-neighbor 3D-gridding process within RockWorks2004 called horizontal lithoblending. This is a cell-based modeling approach where solid-model cell nodes are sequentially assigned properties by looking outward horizontally from each borehole in search circles of ever-increasing diameter. The approach is a simple spatial interpolation method that does not consider spatial structure of the data. Cell dimensions for the modeling were 1,000 m in the horizontal dimension and 10 m in the vertical dimension. The algorithm assigns the lithology values from the borehole data in each vertical interval to cells immediately surrounding each borehole. Then the interpolation moves out by a cell and assigns the next "circle" of cells a lithology value for each vertical interval. The interpolation continues in this manner until the program encounters a cell that is already assigned a lithology (presumably interpolating towards it from an adjacent borehole), in which case it skips the node assignment step. The interpolated data in the resulting solid model have the appearance of stratigraphic units, with aspect ratios that emphasize the horizontal dimension over the vertical. 3D modeling of the borehole data results in the extrapolation of lithologic data throughout a rectangular solid. For visualization purposes, the upper surface of this solid is clipped to the topographic surface by intersecting the solid volume with a DEM and the bottom of the solid volume is intersected with the modeled surface representing the depth to pre-Cenozoic rocks (Blakely and others, 1999; Blakely and Ponce, 2001), resulting in the depiction of the Cenozoic basin fill in the Amargosa Desert basin.

Interpreted depositional environments were modeled in three dimensions as an interpreted-facies solid model that was created by assigning numerical values to each facies class and contouring the values in three dimensions using an inverse-distance algorithm. In this case, the goal was to produce broad, smoothly varying facies trends rather than mimic stratigraphic horizons. In this model, the facies value of each cell is assigned based on the weighted average of neighboring data points; the value of each data point is weighted according to the inverse of its distance from the cell. In this method, distant control points have a lesser influence on the assignment of the facies value to each cell. During the interpolation, a weighting factor of two was used in the inverse distance algorithm. In addition, the interpolation was done using an anisotropic algorithm, where the inverse-distance method searches specifically at the closest point in each 90-degree zone around the cell when assigning the cell value. The borehole data were also declustered so as to minimize the effects of nonuniformly spaced holes. As with the 3D lithology model, for visualization purposes, the upper surface of the 3D solid model is clipped to the topographic surface by intersecting the solid volume with a DEM and the bottom of

Table 2. Descriptive units used in 3D lithology and interpreted facies models. Complex and inconsistent nomenclature used by drillers was simplified to an interpreted lithology so data from many sources could be used in the lithologic model.

Driller's nomenclature	Interpreted lithology (used in 3D lithology model)	Interpreted facies (used in interpreted-facies model)
Boulders; boulders and gravel; gravel; limestone/dolomite slide block; rock	Gravel	Proximal alluvium
Alluvium; boulders and clay; boulders and sand; caliche (when interbedded with sand and gravel); gravel and clay; sand and rock; sand, gravel, and cobbles; sandy gravel; soft caliche	Sand and gravel	Mid-slope alluvium
Clayey, gravelly sand muddy; conglomerate; muddy gravelly sand; muddy sandy gravel; sand, gravel, and clay; sand, clay, and boulders; sand, clay, and gravel; sandy gravel with some silt; silty sand and gravel; soil, unconsolidated conglomerate	Sand, clay, and gravel	Distal alluvium
Sand, clay, and some gravel; clayey gravelly sand, gravelly sand with some silt	Sand, clay, and trace gravel	Sheetwash and (or) eolian interfingered with alluvium
Gravelly sand; sand and some gravel; sand with lenses of gravel	Sand and trace gravel	Sheetwash and (or) eolian interfingered with alluvium
Sand; sandstone	Sand	Sheetwash and (or) eolian
Muddy sandstone; loam; silt and clay; silty sandstone	Sand and clay	Playa or palustrine
Clay, sand, gravel; reworked coarse tuff; sandy clay and gravel	Clay, sand, and gravel	Playa and (or) palustrine interfingered with alluvium
Clay, sand, and trace gravel; gravelly, sandy mudstone; sandy silt and a trace gravel	Clay, sand, and trace gravel	Playa and (or) palustrine interfingered with alluvium
Clay with gravel beds; clay with trace gravel; clay and boulders; clay and rock; gravelly clay; sandy siltstone	Clay and gravel	Playa and (or) palustrine interfingered with alluvium
Clay and silt; marl (calcareous clay and sand); mudstone; reworked tuff; sandy clay; sandy shale; sandy siltstone; siltstone; silty clay; silty mudstone	Clay and sand	Playa
Bentonite; blue clay; clay; claystone; hard pan; mudstone; shale	Clay	Playa
Interbedded claystone, siltstone and (or) sandstone with limestone; limestone, sandy clay; mudstone and marl; sand, clay, limestone; white lime, sand and clay	Clay, sand, and limestone	Playa or palustrine with limestone
Same as clay, sand and limestone with a gravel component described; lime and gravel (when interbedded with fine-grained clay and limestone)	Clay, sand, gravel and limestone	Playa and (or) alluvium interfingered with palustrine
Clay and broken lime; brown clay and white rock; caliche (when interbedded with clay); clay and caliche; clay and limestone; clay and shell; clay with caliche beds; lime (when interbedded with clay); lime and clay; lime shale; limestone and clay	Clay and limestone	Playa or palustrine with limestone
Caliche (when interbedded with bedrock); cemented rock (when interbedded with bedrock); hard lime; hard shell; lime (when interbedded with clay); lime shell; white lime	Limestone	Playa or palustrine with limestone
Basalt or basaltic andesite; black pumice; black rock; black volcanic rock; cinders; lava; obsidian; reddish volcanic sand	Basalt	Basalt or andesite or dacite
Alluvial gravel composed of basalt; black sand	Basalt, alluvial sand, and gravel	Basalt or andesite or dacite
Lava	Andesite and (or) dacite	Basalt or andesite or dacite
Welded tuff, dark-colored rock, cherty tuff, tuff	Welded tuff	Welded or nonwelded tuff
Ash, ash-rich or light-colored tuffs	Nonwelded tuff	Welded or nonwelded tuff
Consolidated Paleozoic limestone, may include some quartzite or shale	Dolomite and (or) limestone	Dolomite or limestone

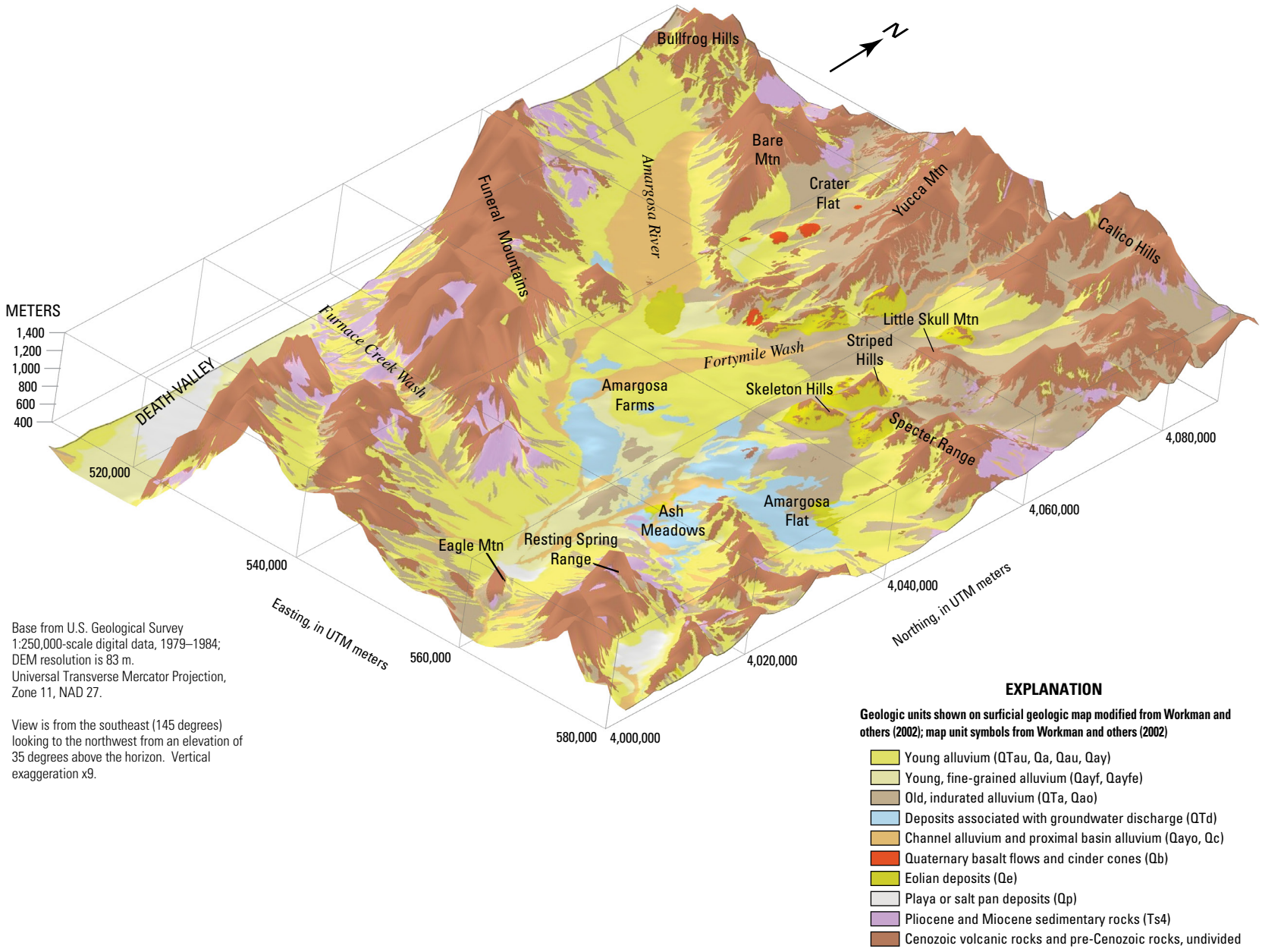

Figure 6. 3D perspective view showing generalized geologic map of the Amargosa Desert basin that emphasizes Quaternary surficial geologic units draped over a digital elevation model.

the solid volume is intersected with the modeled surface representing the depth to pre-Cenozoic rocks (Blakely and others, 1999; Blakely and Ponce, 2001).

A 3D solid model was also created from the vertical resistivity data that were compiled for 79 locations in the basin (Greenhaus and Zablocki, 1982; Senterfit and others, 1982). The model was centered on the Fortymile Wash area and includes parts of Yucca Mountain and the northern part of the Amargosa Desert basin, but is smaller in areal extent than the lithology or interpreted-facies models. The 3D resistivity model was created using an inverse-distance algorithm similar to that used for the interpreted-facies model.

Each of the solid-modeling methods used have inherent limitations that affect the resulting solid models. The horizontal lithoblending method used to construct the 3D lithologic model is sensitive to the amount of data available; data from the deepest boreholes tend to over-extrapolate. Cell values deep in the model tend to be dominated by the few deep boreholes; the deepest parts of sections cut through the model have a distinct striped appearance that is an artifact of this method. However, the areas of greatest interest are the shallower parts of the model where data are more abundant. In the construction of the interpreted-facies model where numeric values were assigned to each facies, the 3D contouring of numerical values results in a continuous series of contours inserted between a high value and a low value. The resulting maps feature artificial halos where facies environments that have very different numerical values are adjacent to each other. For computational efficiency, both the lithologic and interpreted-facies models ignored the effects of stratal dip. The resulting solid models portray the spatial distribution of lithology and facies without any attempts at unit correlation or extrapolation based on unit dip. Pliocene–Pleistocene strata within the basin that are of greatest interest from a groundwater perspective are generally subhorizontal (Denny and Drewes, 1965). Faults were not explicitly included in the creation of these solid models, due to the limitations of the software package used. The interpolation methods used here approximate fault truncations of lithologic units where data density is high.

3D Modeling Results

The 3D lithology model, the 3D interpreted-facies model, and the resistivity model were used to construct cross sections and fence diagrams. Both vertical and horizontal cross sections were created.

3D Lithology Model

The upper surface of the solid volume 3D lithology that is clipped to the topographic surface (fig. 7) generally resembles the surficial geologic map (fig. 6), especially where topographic relief is low and borehole density is high, such as in the center of the Amargosa Desert basin. The surficial geology was not used in the creation of the model; it is an independent dataset and serves as a check on the validity of the model in the shallow subsurface. There is less correspondence in areas of high relief and sparse borehole control (fig. 7). Sparsely distributed boreholes near the boundaries of the model, such as at Yucca Mountain and the Bullfrog Hills (fig. 7), did not sample the highest elevations, so the borehole-based top of the 3D lithology model differs significantly from the higher-resolution DEM, resulting in uncolored regions where Cenozoic rocks are absent in the model. Similarly, the outcrop distribution of pre-Cenozoic rocks is underrepresented when the 3D lithology model is clipped to land surface (fig. 7). In areas where pre-Cenozoic rocks crop out, differences in elevation between the DEM and the more generalized surface representing the elevation of pre-Cenozoic rocks result in a slight over-extrapolation of the modeled extent of the Cenozoic units (fig. 7).

Despite these limitations, a large number of geologic elements present at the clipped upper surface of the 3D lithology model (fig. 7) can be correlated with the surficial geologic map (fig. 6). Cenozoic volcanic rocks in the southern parts of Yucca Mountain and the Bullfrog Hills, at Little Skull Mountain, and in Furnace Creek Wash are portrayed in the model. Coarse-grained sand and gravel deposits of the Amargosa River and Fortymile Wash alluvial channels are well-represented by the 3D model. Widespread deposits of fine-grained sedimentary rocks portrayed in the 3D model in the vicinity of Ash Meadows and Amargosa Flat (fig. 7) correspond well with mapped surficial deposits of paleogroundwater discharge deposits in the south part of the basin (fig. 6).

A series of vertical north-south and east-west sections cut through the 3D lithology model portray the major lithologic variations within the Amargosa Desert basin (fig. 8). Vertical sections are cut through the 3D lithology model at 10-km intervals. Mountainous regions that are underlain by pre-Cenozoic rocks around the basin margins, such as at Bare Mountain, the Funeral Mountains, and the Specter Range, are uncolored (fig. 8). The north end of the model is dominated by welded and nonwelded tuffs of the southwestern Nevada volcanic field near Yucca Mountain (pinks, fig. 8). These volcanic units interfinger with coarse-grained Tertiary and Quaternary deposits (brown, fig. 8) at the northern edge of the Amargosa Desert basin. South of the interface with volcanic rocks and in the vicinity of the Amargosa Farms, the sedimentary basin fill in the northern part of the Amargosa Desert basin has a complex layering of sands and gravels at the surface with fine-grained sand and clay deposits at depth (fig. 8). South of the Amargosa Farms area, the southern part of the basin is filled with an essentially uniform accumulation of fine-grained clay-dominated deposits (blue, fig. 8). In the southwest part of the model domain in the vicinity of Furnace Creek Wash, basalt, andesite, and tuff of the central Death Valley volcanic field interfingers with generally coarse-grained sedimentary deposits.

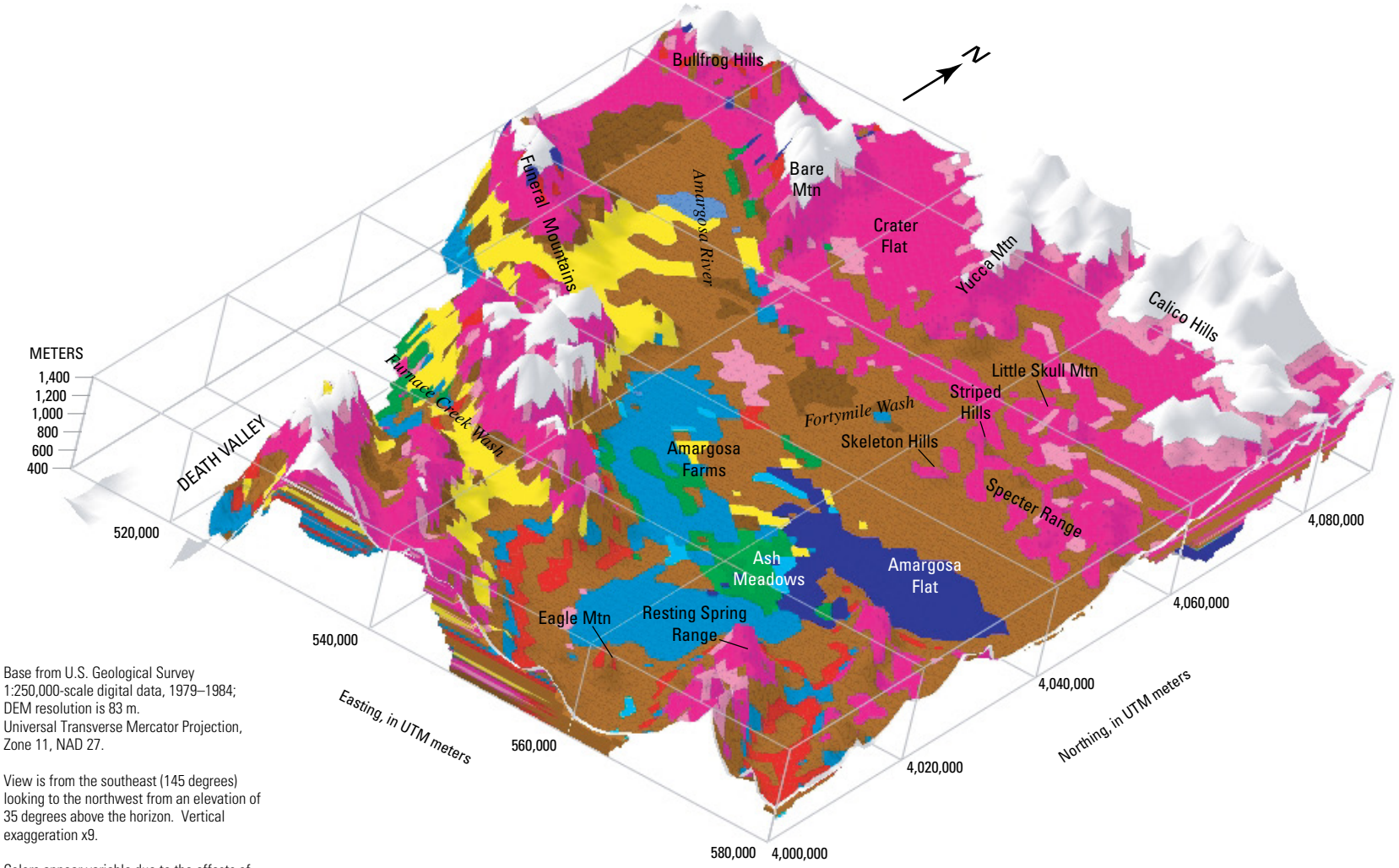

Base from U.S. Geological Survey
1:250,000-scale digital data, 1979–1984;
DEM resolution is 83 m.
Universal Transverse Mercator Projection,
Zone 11, NAD 27.

View is from the southeast (145 degrees) looking to the northwest from an elevation of 35 degrees above the horizon. Vertical exaggeration x9.

Colors appear variable due to the effects of illumination from below and southwest.

Figure 7. 3D perspective view of 3D solid lithology model where the upper surface of 3D lithology model is clipped at land surface with digital elevation model.

Figure 7—Continued. 3D perspective view of 3D solid lithology model where the upper surface of 3D lithology model is clipped at land surface with digital elevation model.

3D Interpreted-Facies Model

Horizontal sections cut through the 3D interpreted-facies model are portrayed in perspective (fig. 9) and plan view (figs. 10*A*–10*E*). In plan view, low-elevation regions in the central and south part of the model fall below the 750-m, 700-m, and, for small areas, the 600-m elevations (figs. 10*A*, 10*B*, and 10*C*, respectively), and thus appear as blank areas of no data. At each elevation, regions inferred on the basis of the gravity inversion to be occupied by pre-Cenozoic rocks are shown as gray polygons. No borehole data were used from Death Valley or the lower reaches of Furnace Creek Wash in the southwest part of the model area. This area of no data is labeled at each elevation and divided from the modeled borehole data by a dashed line; modest over-extrapolation of modeled data south and west of this demarcation line is evident at all elevations. In perspective view, all of the above regions are shown as white, with only the modeled basin-fill units portrayed in color (fig. 9).

At the 750-m elevation (fig. 10*A*), the north-central part of the model is dominated by the welded and nonwelded tuffs and basalts of the southwestern Nevada volcanic field in the volcanic highlands of Yucca Mountain and the Calico Hills. The volcanic rocks are bordered by playa and palustrine deposits, which are primarily localized paleospring deposits. Facies patterns in the vicinity of Yucca Mountain in the north-central part of the model are very generalized and are the result of the very small number of boreholes from this area that were incorporated into the model. Bare Mountain, the Funeral Mountains, and the Specter Range are bordered by coarse alluvial fan material. A coarse-grained, proximal alluvium facies that lies due west of the Specter Range is the alluvial channel of Fortymile Wash. The northwest-striking, coarse-grained deposits south of Bare Mountain are deposited primarily by the active Amargosa River drainage. Most of the central and southern parts of the model area lie below 750 m in elevation and thus do not intersect this surface.

The 700-m elevation (fig. 10*B*) portrays the complexity of the alluvial-channel drainages in the northern part of the Amargosa Desert and the interface of basin-fill sediments with Miocene volcanic rocks at Yucca Mountain. The location of modeled, localized buried basalt centers compares favorably to those inferred from aeromagnetic anomalies (Langenheim, 1995; O'Leary and others, 2002). Most of the southern part of the Amargosa Desert lies below 700 m and the model volume is not intersected.

At the 600-m elevation (fig. 10*C*), the palustrine deposits in the Ash Meadows area are evident in the east-central part of the model. Localized alluvial channels form a complex pattern in the center of the model domain in the vicinity of the Amargosa Farms, but the overall volume of alluvial material is less than at shallower levels and the amount of finer-grained facies is greater. Proximal alluvial-facies rocks in the southern part of the Amargosa Desert basin represent the modern channel of the Amargosa River and local Miocene rocks (Çemen, 1999).

The complex pattern of alluvial facies in the Amargosa Farms area is again seen at the 500-m elevation (fig. 10*D*). Playa and palustrine deposits are well-developed in Amargosa Flat along the east-central part of the model, and in the northern part of the Amargosa Desert basin just south of the volcanic rocks at Yucca Mountain. The lack of alluvium suggests that sediments were deposited in a closed basin—the Amargosa River did not exit the basin. At this elevation, rocks in the Furnace Creek Wash area at the southwestern corner of the model are primarily fine-grained playa and palustrine deposits with rare volcanic rock interbeds.

At the 400-m elevation (fig. 10*E*), playa or palustrine deposits dominate most of the Amargosa Desert basin; the Furnace Creek Wash area in the southwest contains only localized volcanic rocks at this elevation. Coarse alluvial facies extending eastward from the southeastern end of the Funeral Mountains may represent the subsurface projection of east-dipping Oligocene and Miocene rocks that are seen in outcrop (Çemen and others, 1999).

Vertical Sections Cut Through 3D Lithology, Facies, and Resistivity Models

Cross sections were constructed through the 3D solid-volume models of lithology, interpreted facies, and resistivity for selected areas of the Amargosa Desert basin. Figure 11

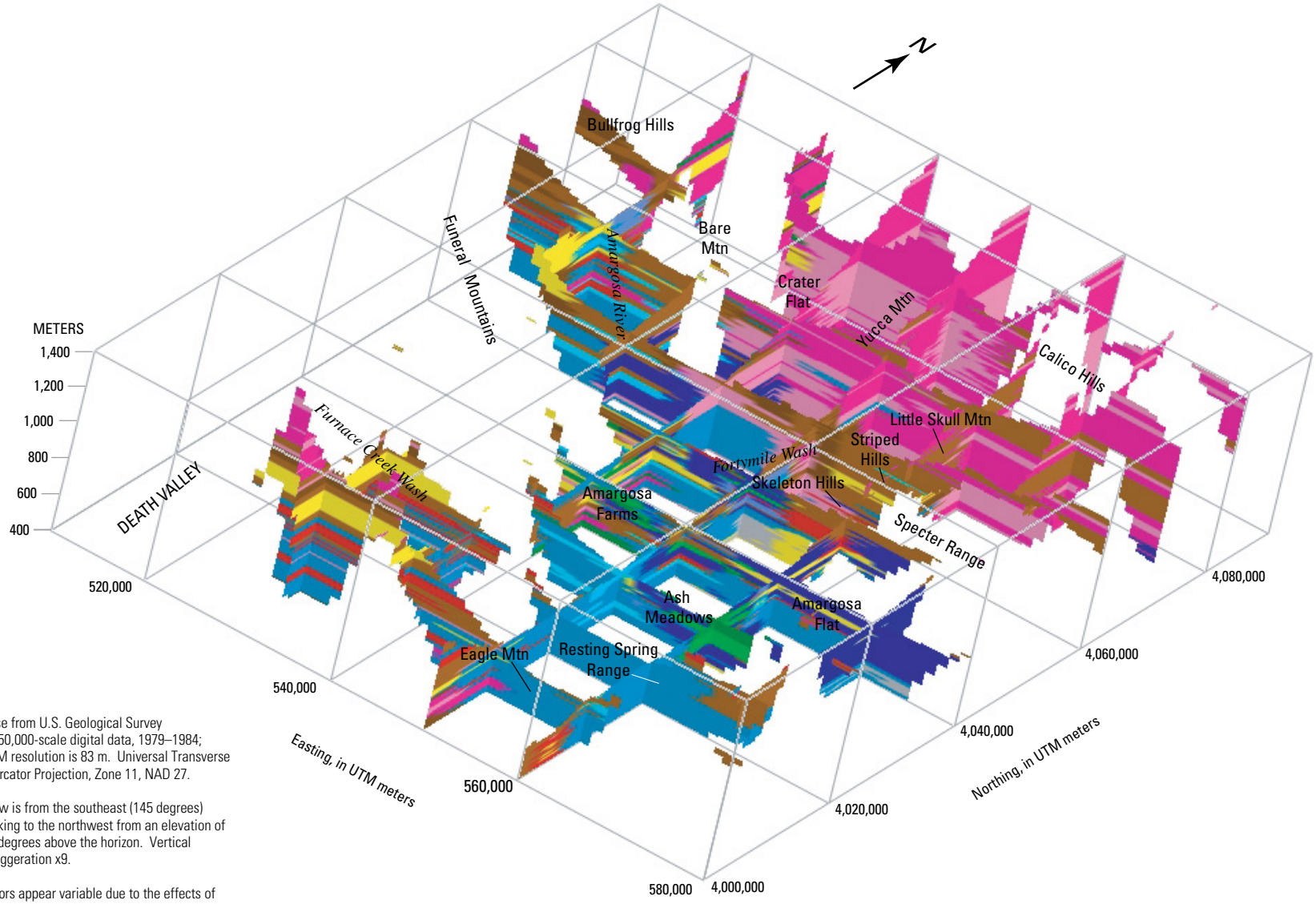

Base from U.S. Geological Survey 1:250,000-scale digital data, 1979–1984; DEM resolution is 83 m. Universal Transverse Mercator Projection, Zone 11, NAD 27.

View is from the southeast (145 degrees) looking to the northwest from an elevation of 35 degrees above the horizon. Vertical exaggeration x9.

Colors appear variable due to the effects of illumination from below and southwest.

Figure 8. 3D perspective view of vertical sections cut through the 3D solid lithology model.

Figure 8—Continued. 3D perspective view of vertical sections cut through the 3D solid lithology model.

shows the locations of the cross sections along with the locations of the well and resistivity data used to create the solid models. The locations of the cross sections were chosen to highlight regions of geologic and hydrologic significance within the basin. Borehole data within a 1-km area on either side of the section were projected onto the cross section model results. In many cases, the modeled lithology along the section differs from the borehole data projected onto the sections, resulting in different geologic units portrayed on the model sections and the projected boreholes.

To aid in visualizing the relation between subsurface geologic units and the groundwater system, a generalized potentiometric map was created by contouring water-level measurements from wells in the Amargosa Desert where head observations were interpreted to represent the regional potentiometric surface (San Juan and others, 2004). Profiles from this generalized potentiometric surface are shown on the vertical sections cut through the lithology and interpreted-facies models. These profiles emphasize the thick unsaturated zone known to be present beneath Yucca Mountain and the very shallow water table beneath most of the Amargosa Desert basin. Regional springs are present at Ash Meadows where the water table intersects the land surface. The clear freshwater supports a variety of wildlife and vegetation. Where spring pools do not form, groundwater discharge occurs in diffuse zones. In some areas, the water is derived from lateral flow at the distal facies of alluvial fans. This palustrine environment traps fine-grained sediments. When dry, these deposits expose fossil-rich silts and clays; soils are not present because these deposits erode too rapidly. Paleodischarge deposits are the geologic record of discharge at these diffuse zones.

The northwest-southeast cross section *FC–FC′* (fig. 12) portrays modeled subsurface lithology in the vicinity of Furnace Creek Wash. This section lies within the Furnace Creek basin (Wright and others, 1999; Fridrich and Thompson, 2011), a synextensional volcano-sedimentary trough closely associated with the Furnace Creek fault zone. The northwestern part of the section portrays shallow basalts (red, fig. 12) and gravels (brown, fig. 12) that correspond to surface outcrops of the Funeral Formation (Wright and others, 1999). Underlying sands and clays that represent fine-grained playa/palustrine deposits with interbedded volcanic rocks likely correspond to the Furnace Creek Formation (Wright and others, 1999). This cross section intersects both the main trace of the Furnace Creek fault and a southern splay, showing abrupt changes in modeled lithology in the vicinity of each fault, such as between buried playa and (or) paleodischarge deposits and buried basalt at the southern splay of the Furnace Creek fault, and between the buried basalt and depositional sand and gravels at the Furnace Creek fault. To the southeast of the Furnace Creek fault zone, the lithology model portrays dominantly coarse sands and gravels (brown) that are a composite of alluvial material shed off of the Resting Spring Range to the east and older, consolidated conglomerates that are exposed at the southeast end of Eagle Mountain (Çemen, 1999).

Cross section *YM–YM′* (fig. 13) is a south-north cross section just east of Yucca Mountain, highlighting the southward transition from the volcanic rocks of the southwestern Nevada volcanic field to the sedimentary rocks to the south. Welded and nonwelded tuffs (pinks on lithology model cross section, fig. 13) at Yucca Mountain transition southward across the Paintbrush Canyon fault to the coarse alluvial gravels (brown on lithology model cross section, fig. 13) of the Fortymile Wash drainage. These gravelly deposits prograde to finer sands and clayey sands, south across the Amargosa Basin. This prograding pattern of alluviation can be observed in both the interpreted-facies and the resistivity model. In the subsurface, the east-west splay of the Gravity fault bounds the south side of a buried ridge of pre-Cenozoic rocks to the west of the Specter Range (fig. 11). Near the south end of the lithology model cross section, basalts (red) that were intersected in the subsurface (Carr and others, 1995) are interbedded within fine-grained basin fill. The modeled resistivity data correspond well with the 3D lithologic model; the smallest resistivity values correspond to coarse-grained alluvial sediments, and the highest resistivity values are associated with the welded tuffs. The resistivity data express a distinct anomaly where the Paintbrush Canyon fault is intersected by the cross section.

The west-east cross section *BC–BC′* (fig. 14) shows the center of the basin in the vicinity of the Amargosa Farms, which has the highest density of shallow well control in the study area. The section crosses the Amargosa River near the west end of the cross section. Near the Amargosa River fault,

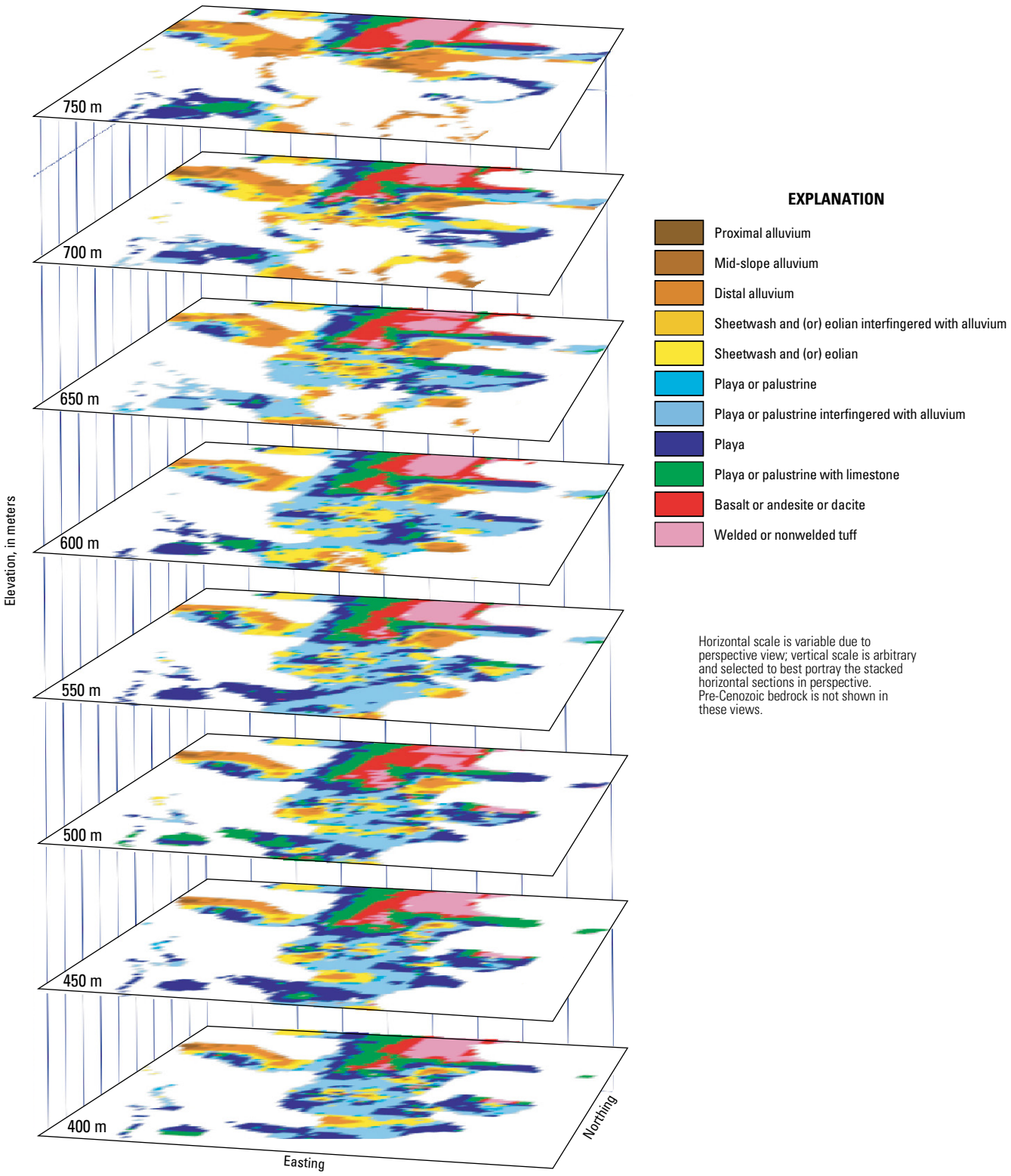

Figure 9. 3D perspective view of horizontal sections cut through 3D interpreted-facies model.

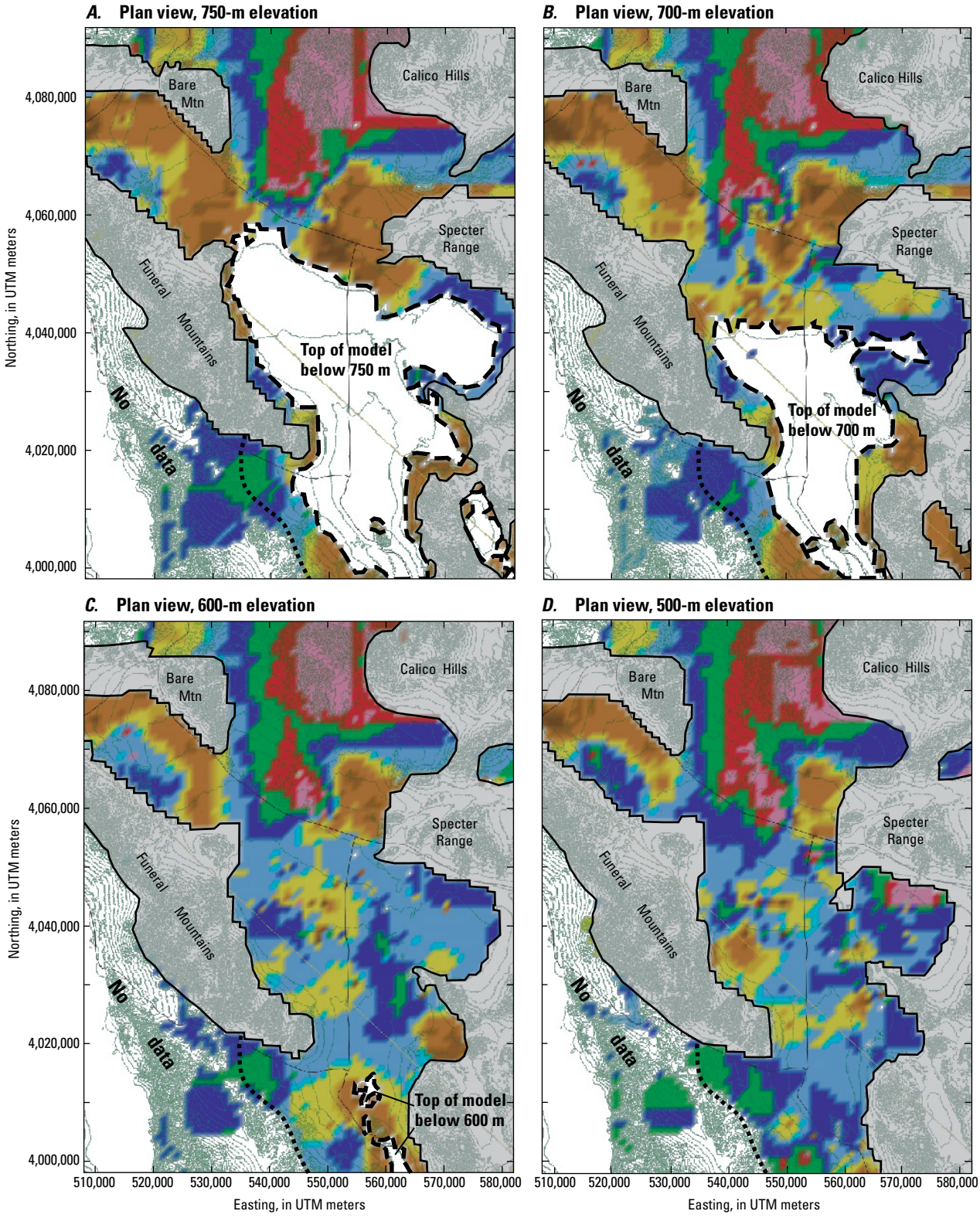

Figure 10. Plan views of sections cut through 3D interpreted-facies model. *A*, 750-m elevation; *B*, 700-m elevation; *C*, 600-m elevation; *D*, 500-m elevation; *E*, Plan view, 400-m elevation.

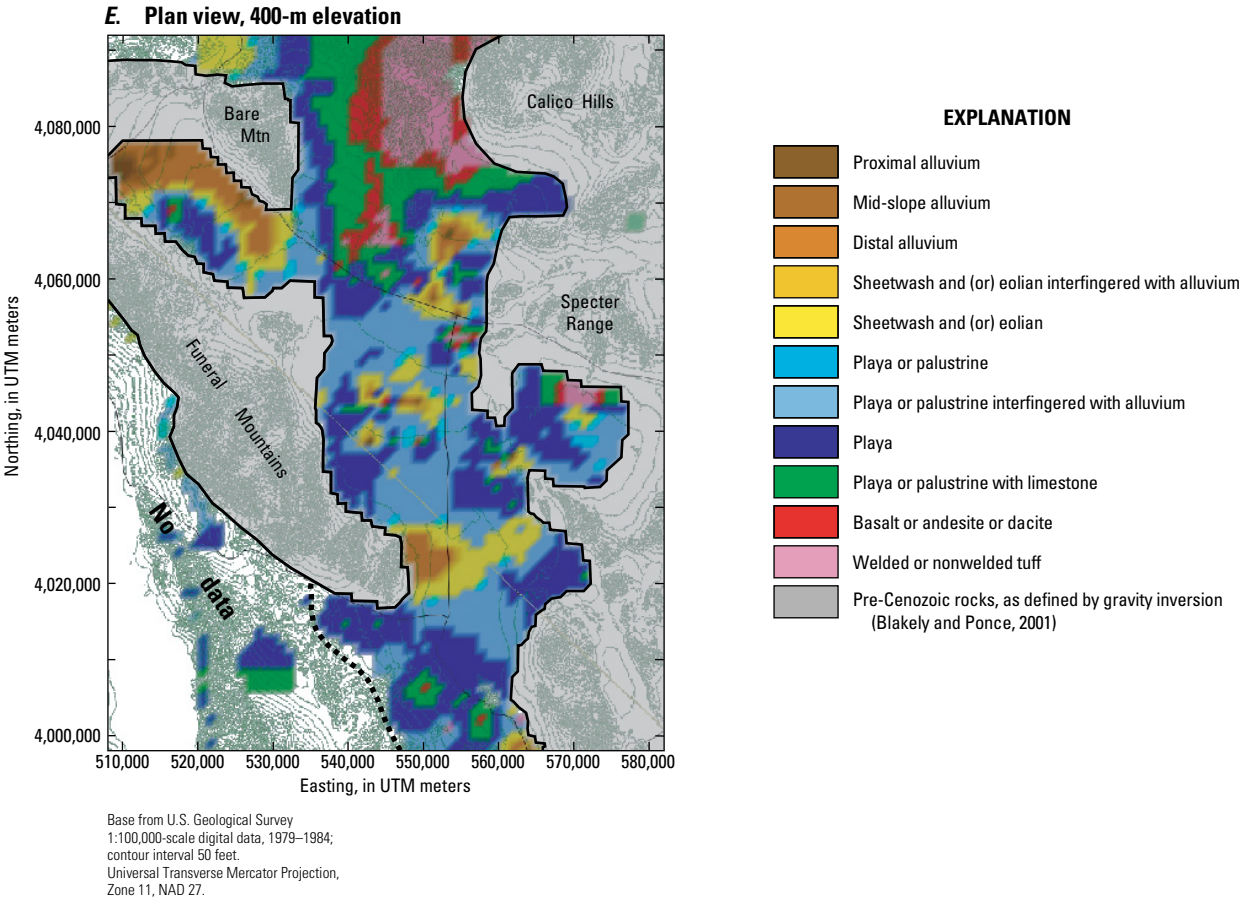

Figure 10—Continued. Plan views of sections cut through 3D interpreted-facies model. *A*, 750-m elevation; *B*, 700-m elevation; *C*, 600-m elevation; *D*, 500-m elevation; *E*, Plan view, 400-m elevation.

coarse gravel and sand occurs in the upper 50 m, overlying finer-grained sand and silty-sand and interbedded volcanic rocks. These buried volcanic rocks on the southwest side of the Amargosa Valley are likely sourced from the central Death Valley volcanic field (Wright and others, 1991). The central part of the lithology model cross section in the Amargosa Farms area depicts complex layering of coarse-grained gravel and sand (brown and yellow, fig. 14) that are primarily alluvial channel and eolian deposits, probably in part paleochannels of the Amargosa River and Fortymile Wash drainages. These sands and gravels overlie fine-grained clay and sand (blue, fig. 14) that are likely playa or palustrine deposits. This cross section intersects the Amargosa River fault and the main trace of the Gravity fault; abrupt changes in modeled lithology are seen in the vicinity of these faults. The Gravity fault is associated with a structural high in the pre-Cenozoic rocks and with buried basalt (red, fig. 14). The resistivity data show a general correspondence to the lithology model, with the largest resistivity values corresponding to intervals dominated by coarse-grained sediments near Fortymile Wash and adjacent to the Gravity fault. Correspondence between the location of large resistivity values, the presence of coarse-grained sediment, and low sodium concentrations in groundwater have been interpreted to reflect the southward flow of dilute ground waters within the coarse alluvial gravels of Fortymile Wash (Oatfield and Czarnecki, 1989).

Cross section *FW–FW′* (fig. 15) is a southwest-northeast cross section along the axis of Fortymile Wash. Like cross section *YM–YM′* (fig. 13), depositional units prograde southward from coarse to fine toward the center of the basin. Fine-grained playa and (or) palustrine deposits are intersected in the center of the basin. On section *FW–FW′*, the coarser sediments in the Amargosa Farms area are probably related to paleochannels of the Amargosa River. The abundance of water wells in the Amargosa Farms area pump from a 150-m-thick package of relatively coarse sediments that are fault-bounded and flanked to the southwest and northeast by fine-grained playa and (or) palustrine deposits (blue, fig. 15).

Resistivity of the alluvium in the Amargosa Desert basin is reported to be controlled by the salinity of groundwater, the degree of saturation, and to a lesser degree, the electrical conductivity of the mineral grains (Oatfield and Czarnecki,

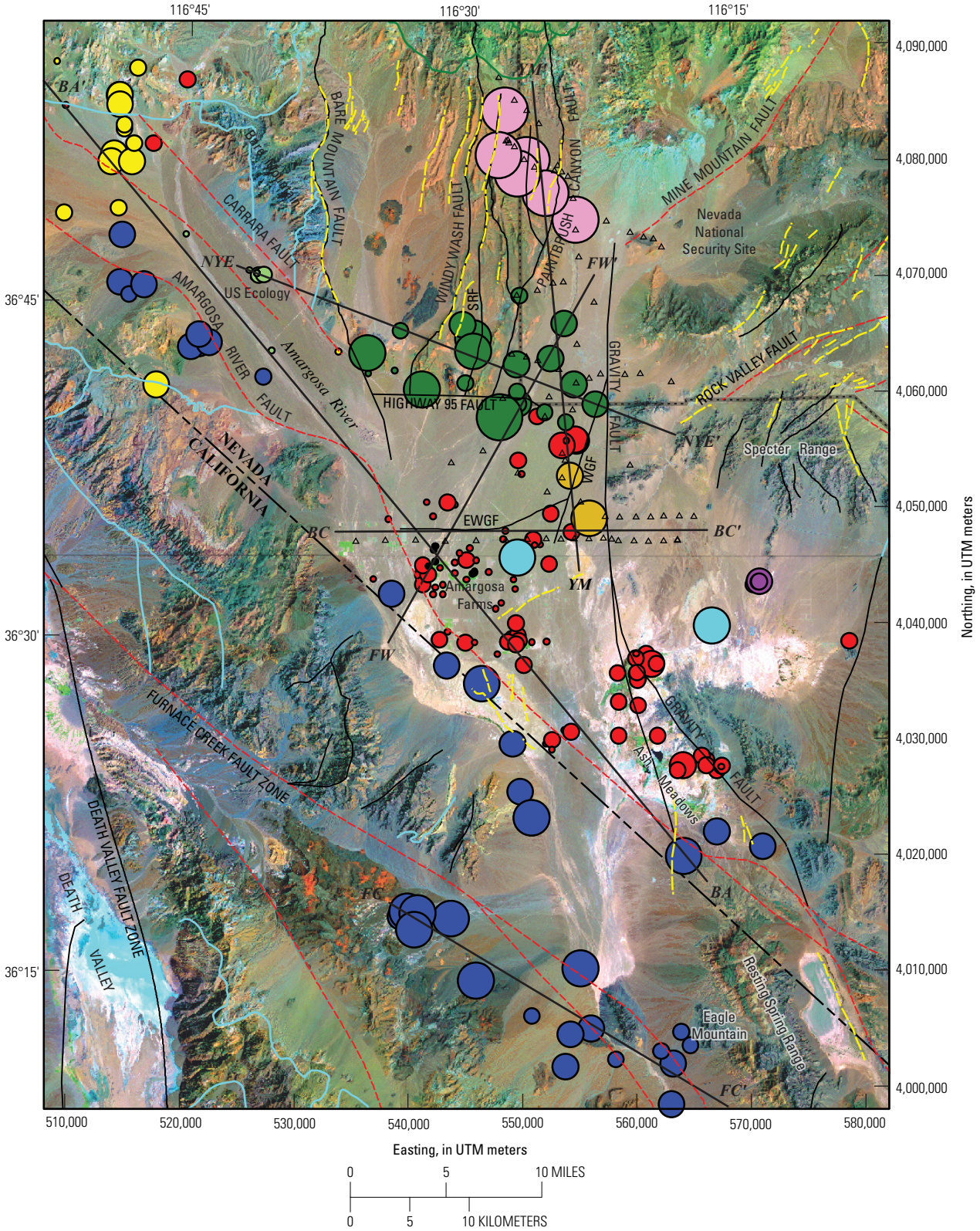

Figure 11. Map showing locations of well and resistivity data and cross sections shown in figures 12–17.

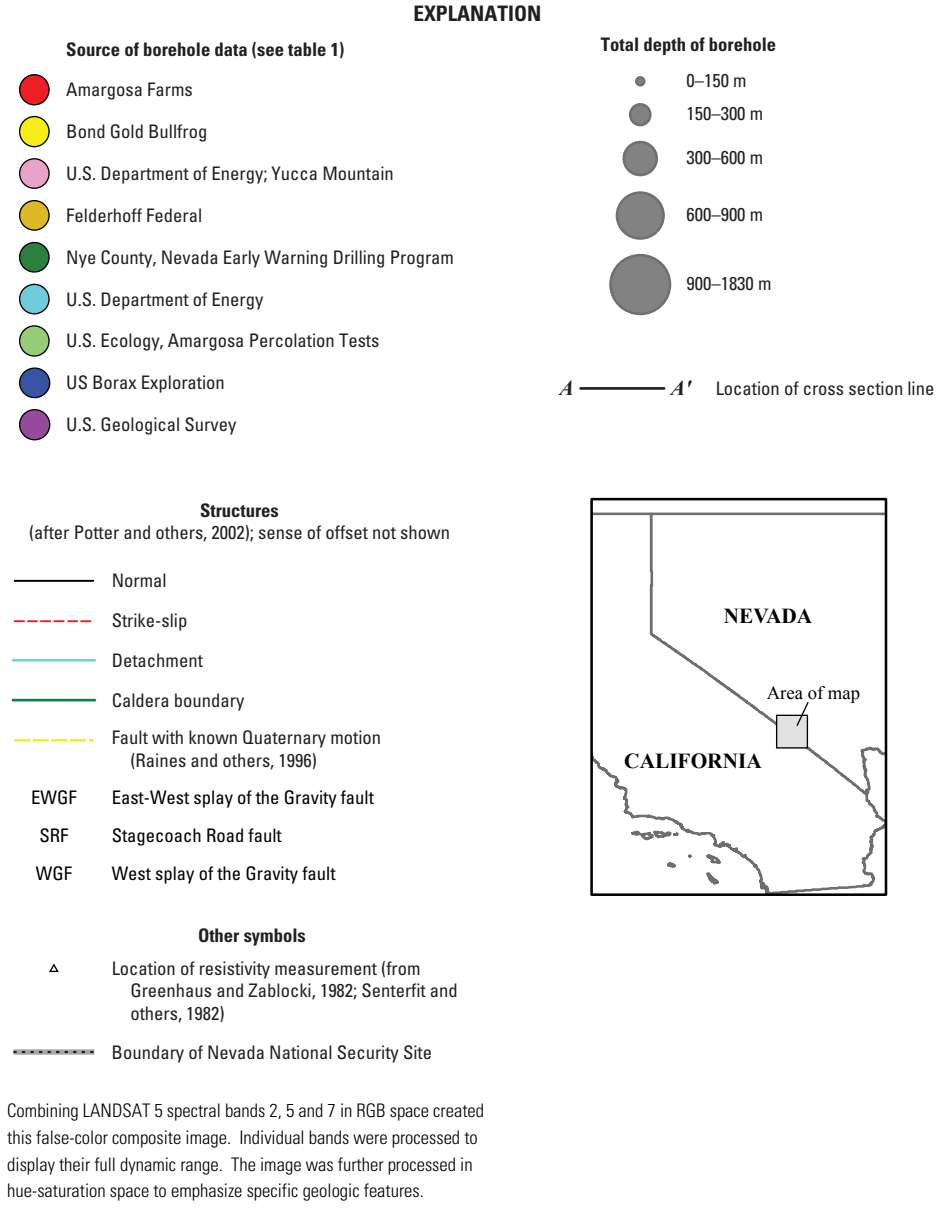

Figure 11—Continued. Map showing locations of well and resistivity data and cross sections shown in figures 12–17.

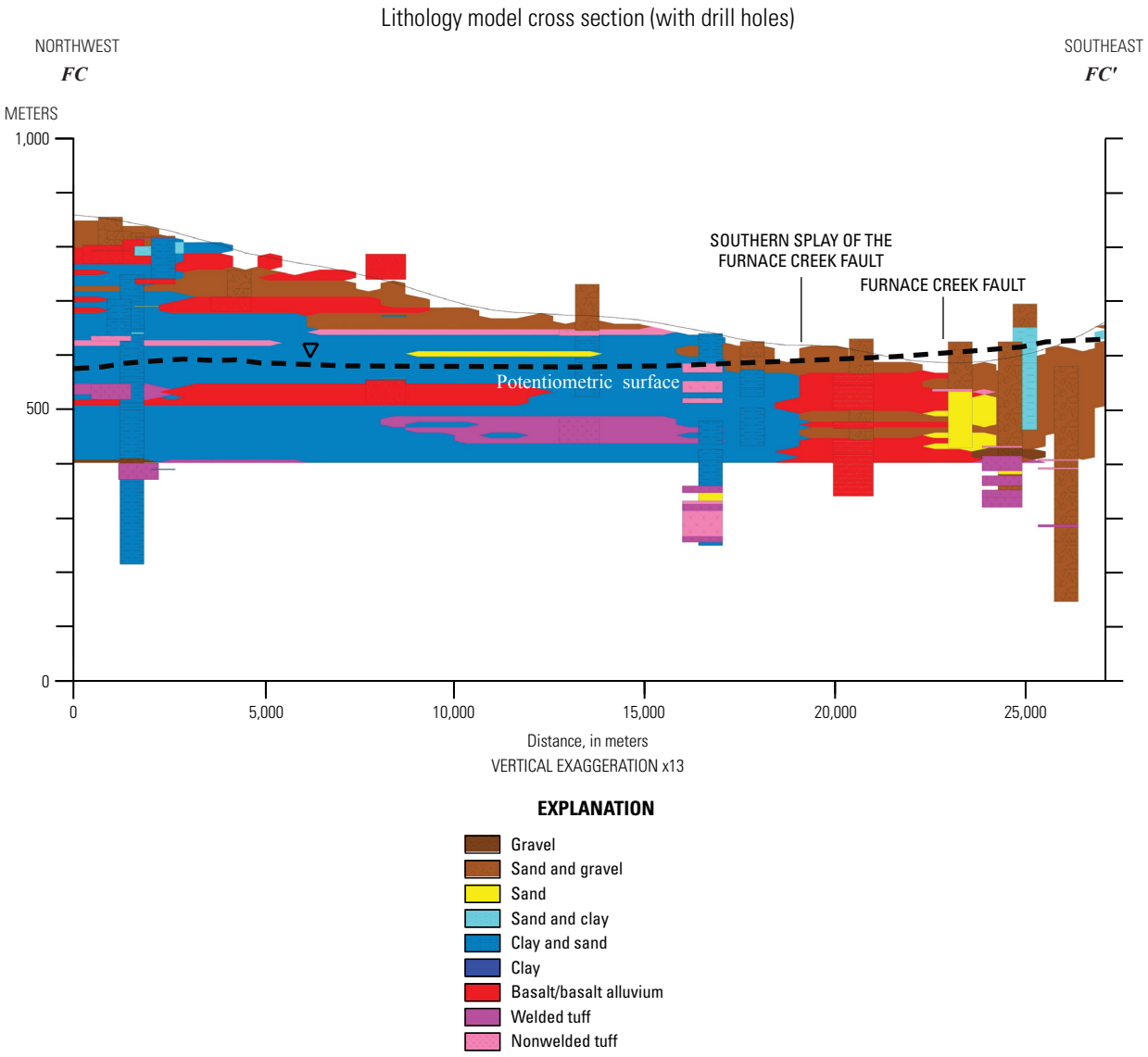

Figure 12. Cross-section *FC–FC'* through the 3D lithology model. Section lies generally south and west of the Furnace Creek fault zone.

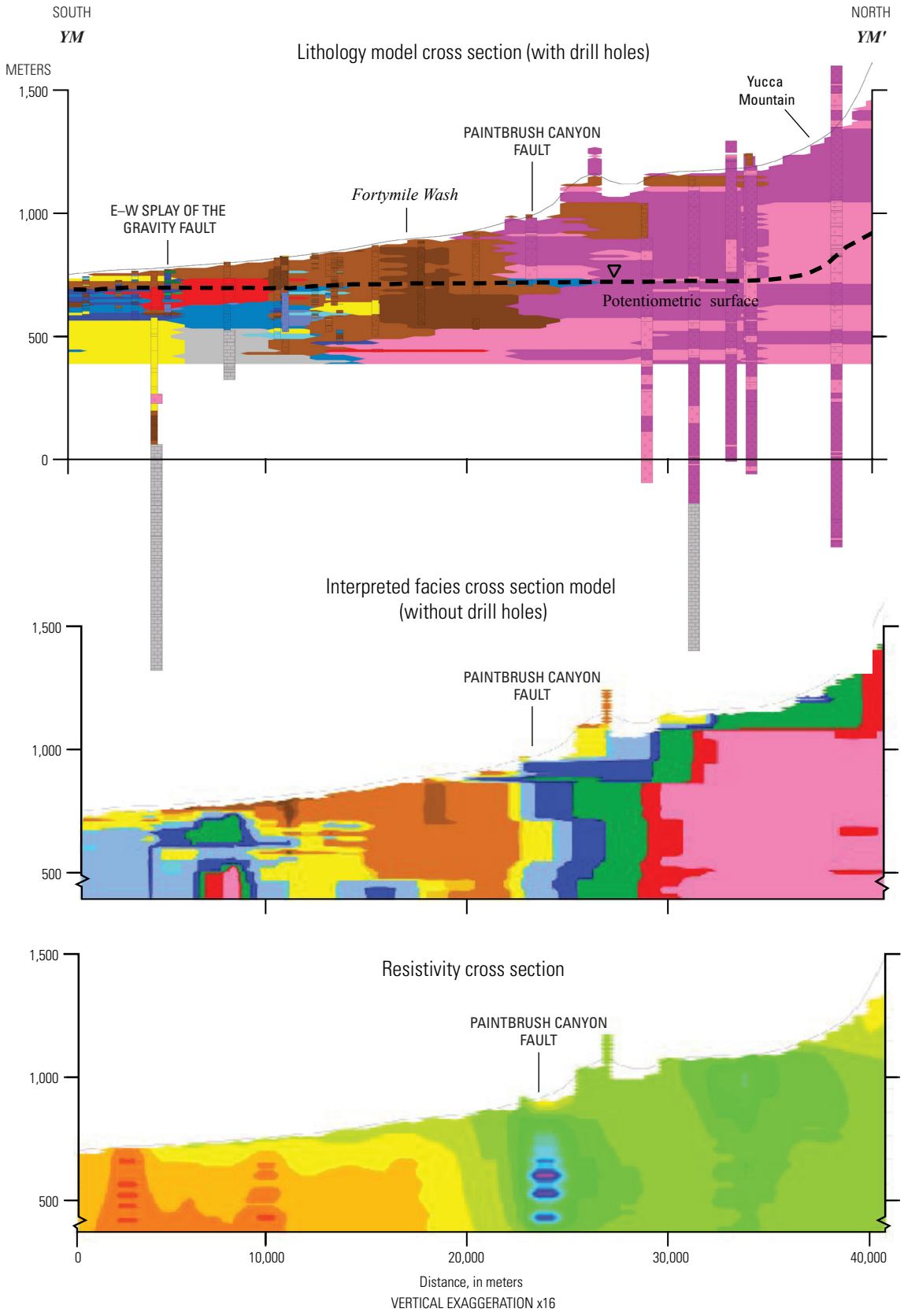

Figure 13. South-north cross section *YM–YM'* through the 3D lithology, interpreted facies, and resistivity models. Section extends from the north-central part of the Amargosa Desert basin to Yucca Mountain.

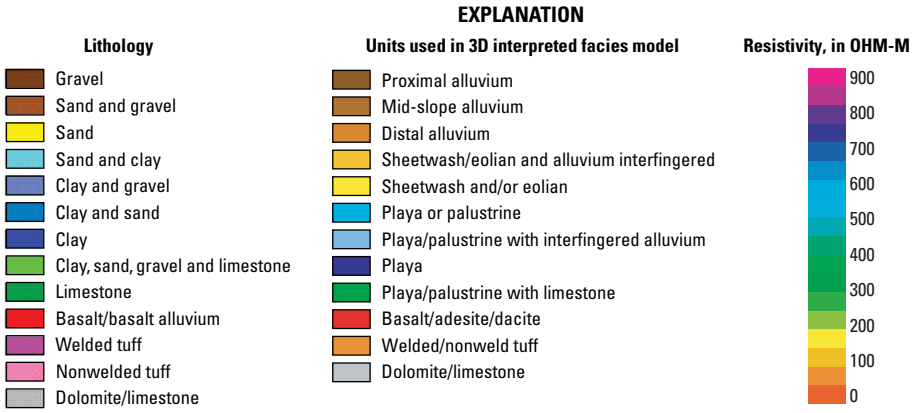

Figure 13—Continued. South-north cross section *YM–YM′* through the 3D lithology, interpreted facies, and resistivity models. Section extends from the north-central part of the Amargosa Desert basin to Yucca Mountain.

1989). The resistivity data show a general correspondence to the lithology model, with the smallest resistivity values corresponding to intervals dominated by fine-grained sediments (fig. 15). Correspondence between the location of large resistivity values, the presence of coarse-grained sediment, and low sodium concentrations in groundwater have been interpreted to reflect the southward flow of dilute ground waters within the coarse alluvial gravels of Fortymile Wash (Oatfield and Czarnecki, 1989).

Section *NYE–NYE′* (fig. 16) incorporates data from wells at the US Ecology site and wells drilled immediately south of Yucca Mountain as part of the Nye County Early Warning Drilling Program. This cross section intersects the major north-south trending faults within and surrounding Yucca Mountain. Monitoring holes drilled south of Yucca Mountain provide detailed data on the relation between sedimentary basin-fill rocks and the Miocene volcanic rocks of the southwestern Nevada volcanic field (Spengler and others, 2006). Although faults were not explicitly incorporated in the lithology model, the closely spaced borehole data result in abrupt lithologic changes in the model results that correspond to the Windy Wash, Stagecoach Road, and Paintbrush Canyon faults (fig. 16). For modeling convenience, lithologic units were allowed to extrapolate across the traces of the Bare Mountain and Carrara faults at the southern end of Bare Mountain; pre-Cenozoic rocks probably occur at shallow depths between these two faults.

The northwest-southeast cross section *BA–BA′* (fig. 17) portrays modeled subsurface lithology along the basin axis of the Amargosa Desert and includes data from the Amargosa Farms area and the southern part of the Ash Meadows area. The southern part of the basin is a thick accumulation of fine-grained clay, sand, and limestone that are interpreted as playa and (or) palustrine deposits (blue, fig. 17). The basin fill northwest of Fortymile Wash is coarse alluvial sand and gravel (brown, fig. 17). This cross section intersects an unnamed fault in the northwestern part of the basin that is well-expressed as sand and gravels offset against Tertiary playa and (or) palustrine limestone and volcanic rock at depth. The Amargosa River fault, coincident with the northeastern edge of a pre-Cenozoic bedrock high in the center of the cross section, has coarse alluvium offset against fine-grained playa and (or) palustrine deposits. These deposits are inferred to be present at depth in the northern part of the basin, buried by younger alluvium.

Multiple Sections Cut Through 3D Lithology Model

Several cross sections (fig. 18) cutting through the 3D lithology model were combined to create fence diagrams that highlight modeled lithology of the northern and central parts of the Amargosa Desert basin (fig. 18). In both fence diagrams, boreholes are shown in perspective view as cylinders that are colored in the same fashion as the lithologic units shown on the cross sections (figs. 19 and 20). In both diagrams, the upper surface of the cross sections and the top of each borehole are plotted at the elevation of land surface; land surface is transparent so that the sections and boreholes appear to hang in space. Faults were not used in the 3D modeling algorithms, but are portrayed as a series of parallel lines for reference (figs. 19 and 20).

In the north part of the valley, cross section *NYE–NYE′* is shown in perspective view with four transverse sections (fig. 19) to illustrate modeled lithologic variations in the northern part of the Amargosa Desert basin and the southern part of Yucca Mountain. Miocene welded and nonwelded tuffs (pink, section *B–B′*, fig. 19) interfinger with alluvial sands and gravels deposited in Fortymile Wash to the east of Yucca Mountain (brown and oranges on the northeast ends of *C–C′* and *D–D′*). The volcanic rocks overlie and interfinger with clays and sand to the south (blues and brown on the southwest ends of *B–B′*

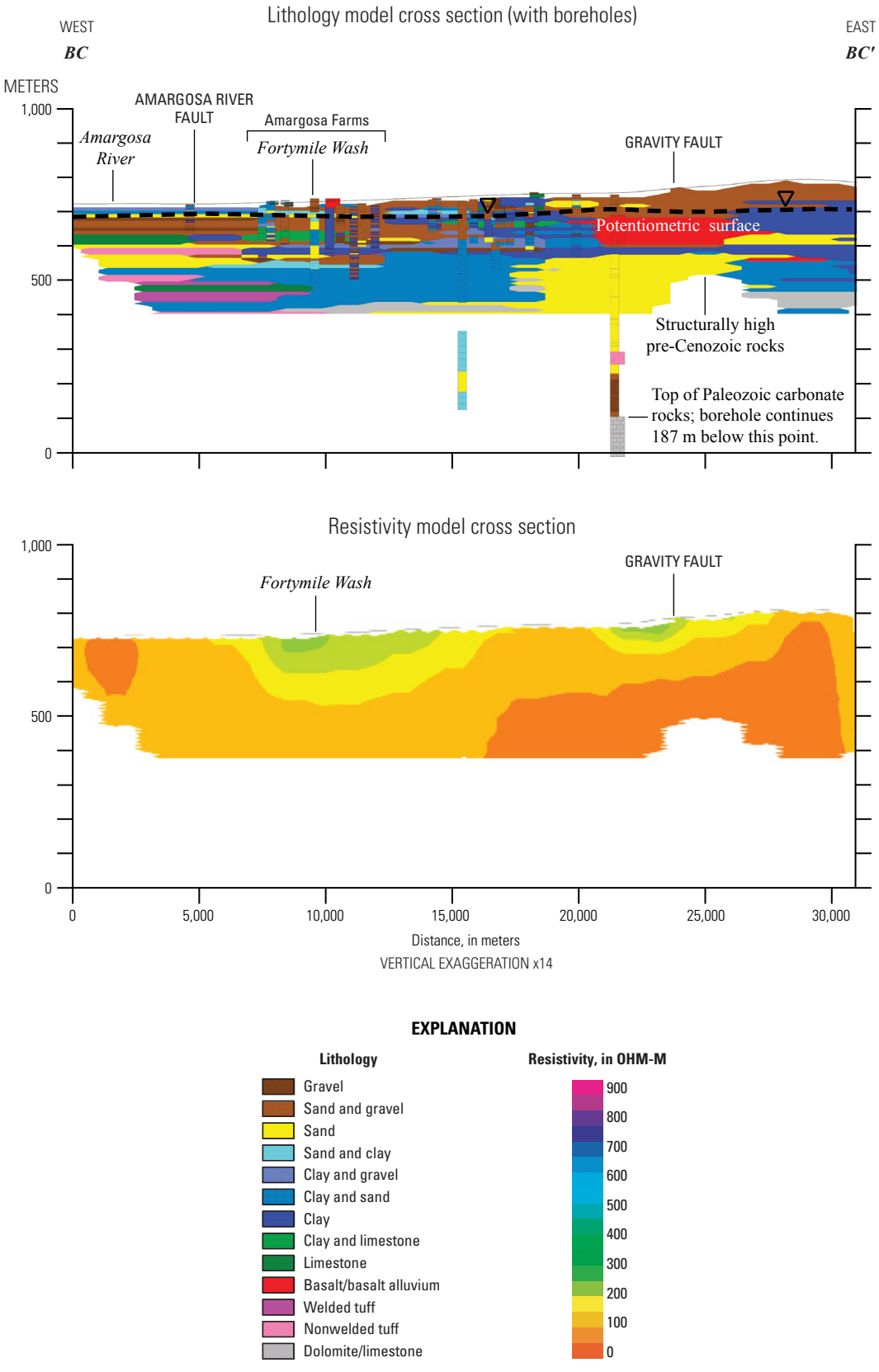

Figure 14. Cross section *BC–BC′* through the 3D lithology and resistivity models. Section crosses the center of the Amargosa Desert basin.

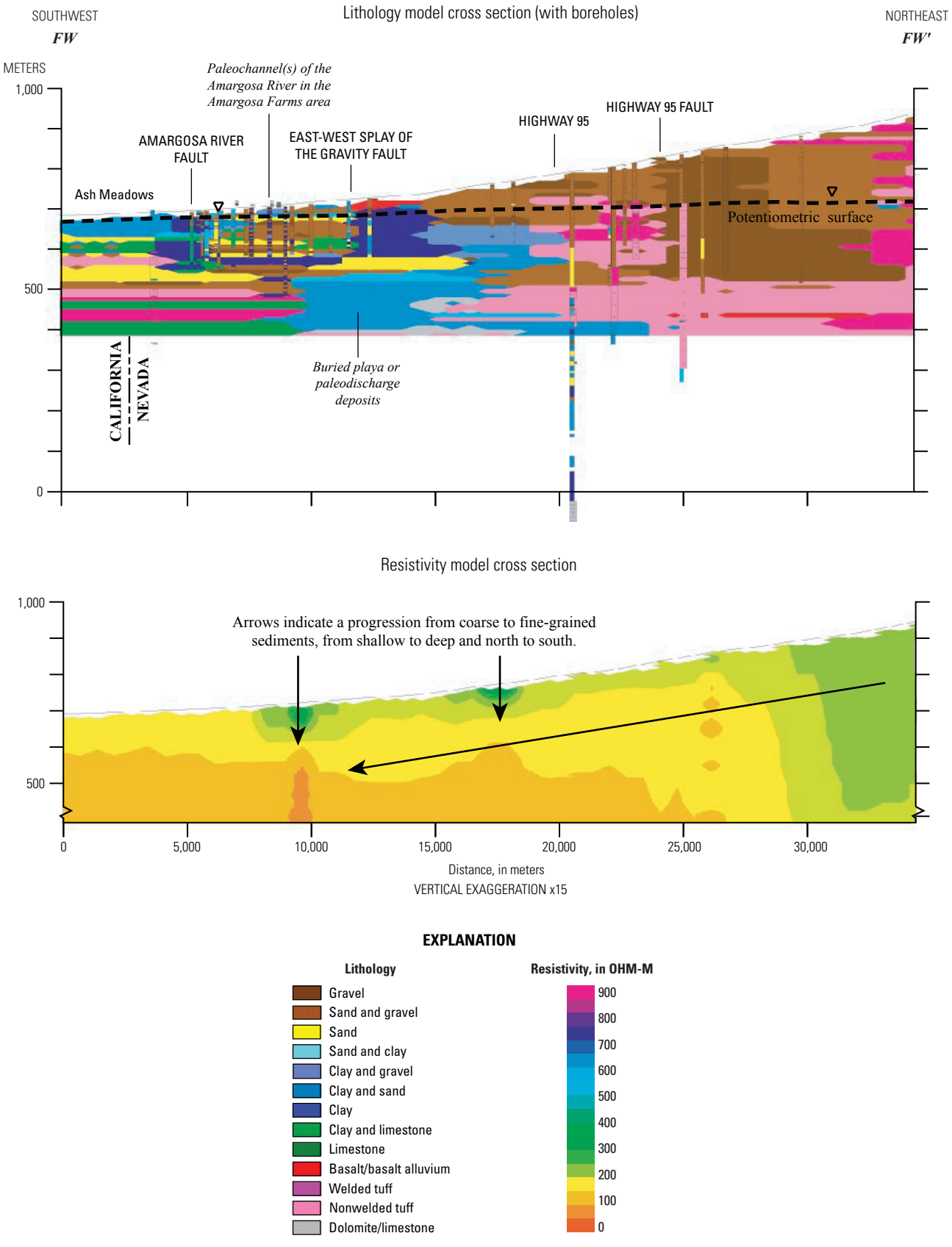

Figure 15. Cross section *FW–FW'* through the 3D lithology model resistivity models. Section is cut along the axis of Fortymile Wash.

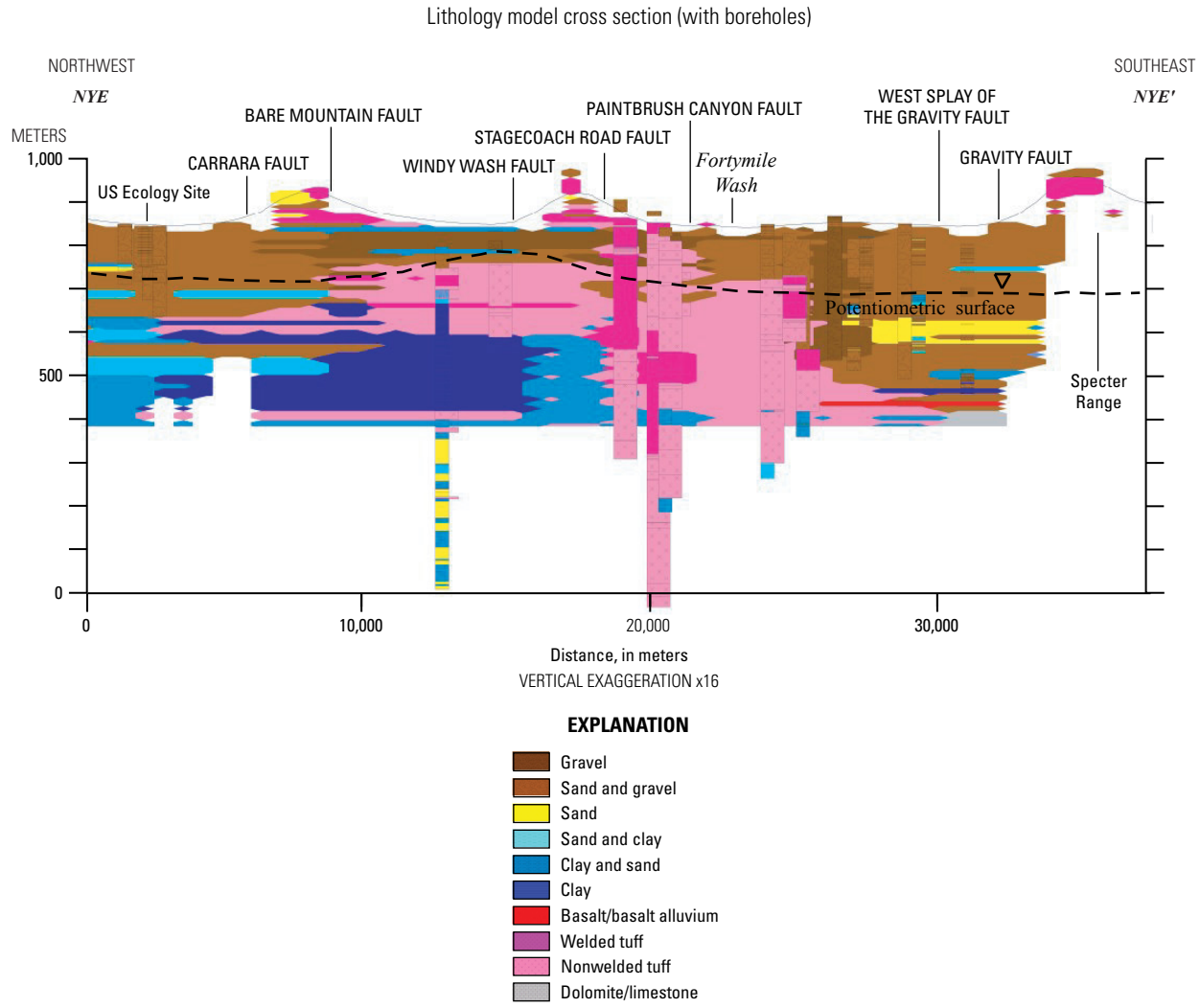

Figure 16. Cross section *NYE–NYE′* through 3D lithology model. Section is located south of Crater Flat and Yucca Mountain.

and *C–C′*, fig. 19) as shown by subsurface data from the Nye County Early Warning Drilling Program (Spengler and others, 2006). Coarse sand and gravel dominate the shallow subsurface in the northwestern part of the area (brown and orange, section *A–A′*, fig. 19). These sediments are underlain by a thick section of sandy clay (blues in the lower parts of section *A–A′* and the northwestern end of *NYE–NYE′*, fig. 19). This deeper fine-grained sequence defines the presence of a closed playa basin prior to the establishment of the Amargosa River drainage in this part of the basin. This playa was eventually overtopped by fine-grained sands deposited by either eolian processes or fluvial reworking.

The north-central part of the Amargosa Desert basin (west end of cross section *I–I′*, fig. 20) has a complex layering of coarse-grained gravels and sands (brown and yellow on *I–I′*, fig. 20) that are primarily alluvial channel and eolian deposits. These aquifers are complexly interfingered with fine-grained confining units that constitute the majority of basin fill in the southeastern part of the basin (blue units on *I–I′*, *H–H′*, and *J–J′*, fig. 20). The location and size of buried basalts (red, fig. 20) generally agree with magnetic anomalies defined by ground and aeromagnetic data (Langenheim, 1995; O'Leary and others, 2002). Abrupt lithologic transitions generally correspond to interpreted locations of faults in the subsurface (Potter and others, 2002), such as the truncated lithologic units near the southern ends of sections *F–F′* and *G–G′* (fig. 20). The southern part of the basin is filled with fine-grained clays and limestone (blue and green units on *I–I′*, *H–H′*, and *J–J′*, fig. 20) that represent playa and palustrine deposits. The broad distribution of these fine-grained deposits in the southern part of the basin preserves the record of an environment much wetter than the modern climate; modern discharge is confined to a considerably smaller area in the vicinity of Ash Meadows (Winograd and Thordarson, 1975).

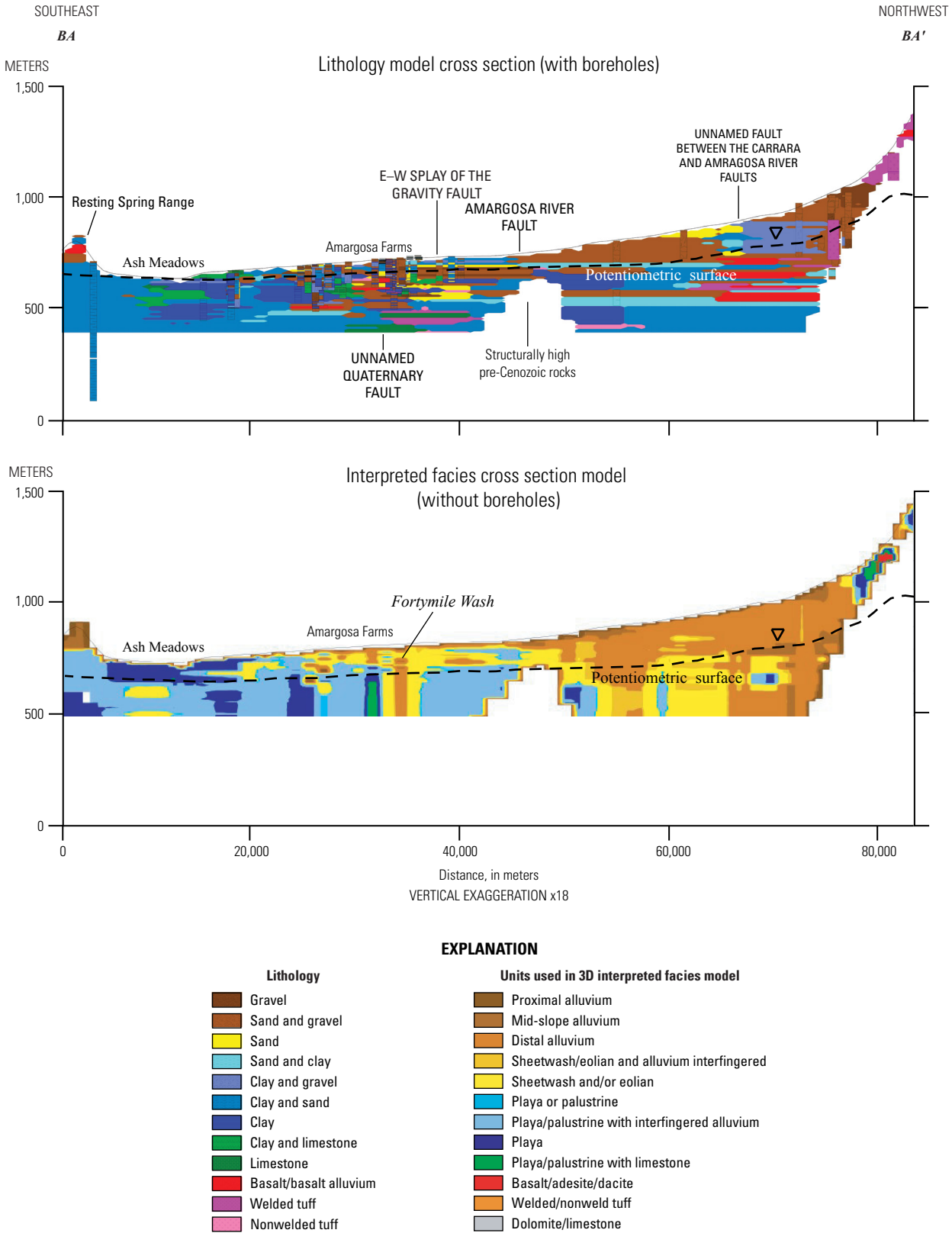

Figure 17. Cross section *BA–BA'* through the 3D lithology and interpreted-facies models. Section extends along the axis of the Amargosa Desert basin.

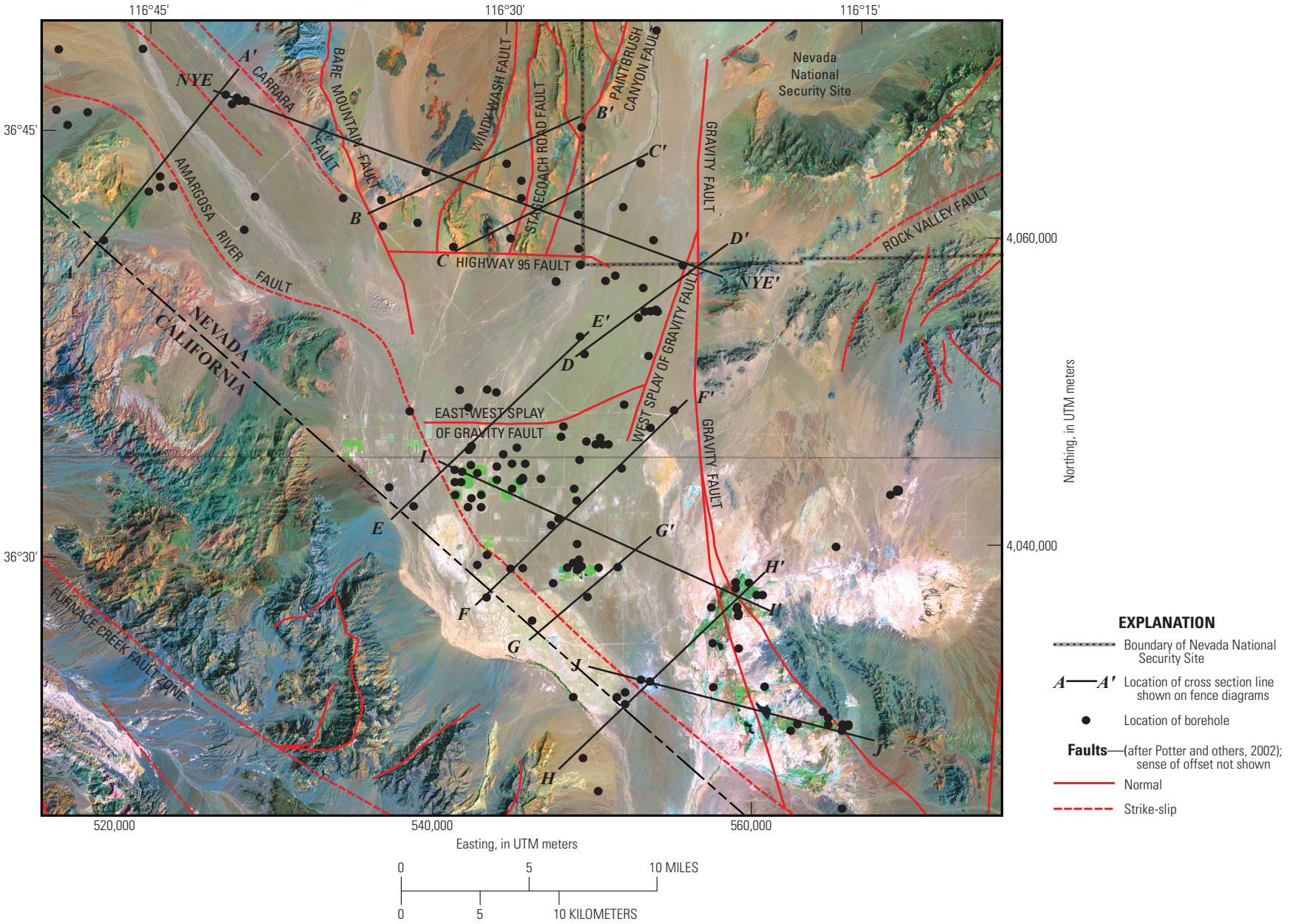

Figure 18. Map showing location of cross sections used to construct fence diagrams shown in figures 19 and 20.

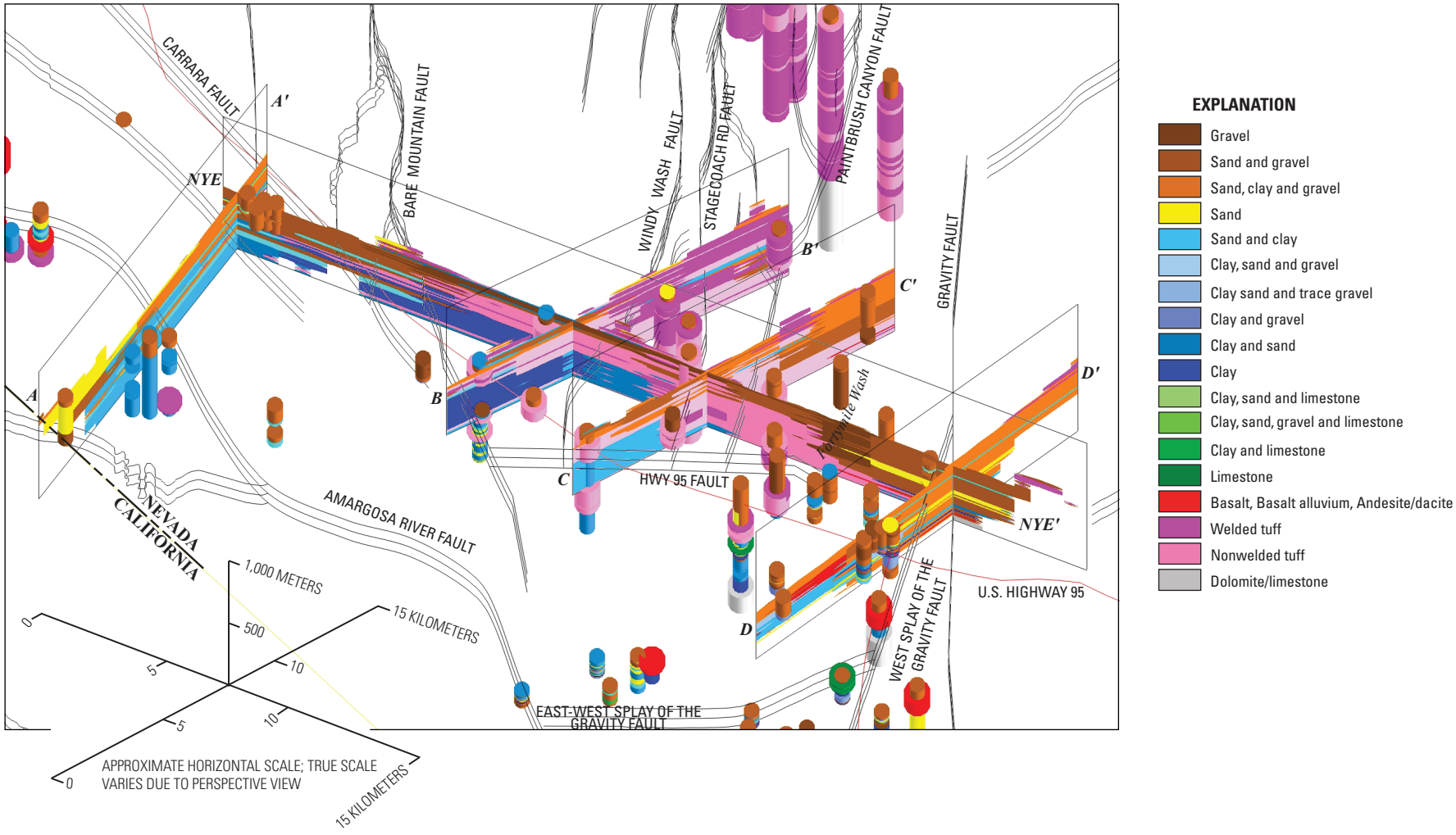

Figure 19. Perspective view of drill-hole data and cross sections cut through 3D lithology model in the northern part of the Amargosa Desert basin and southern part of Yucca Mountain.

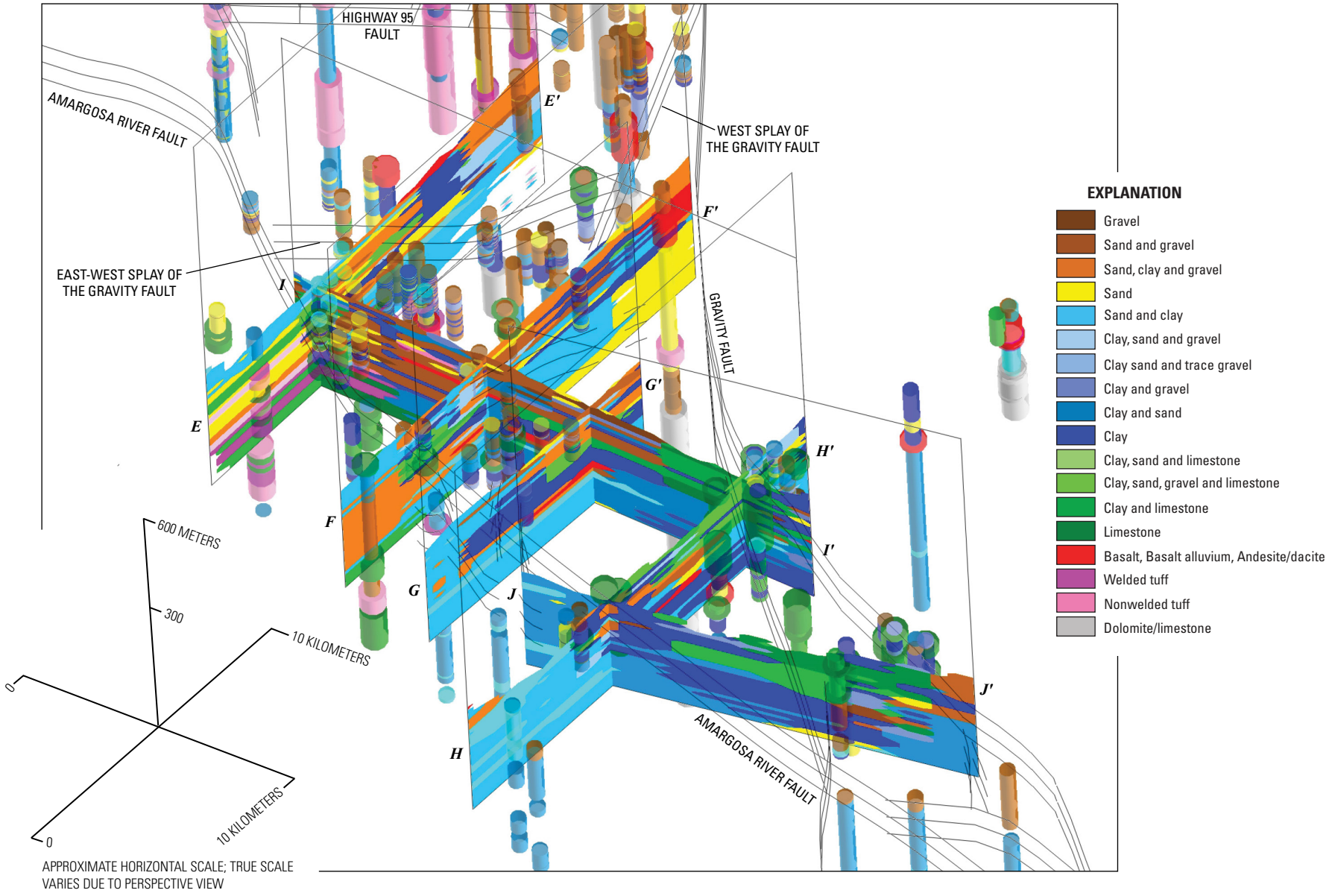

Figure 20. Perspective view of drill-hole data and cross sections cut through 3D lithology model in the central part of the Amargosa Desert.

Summary and Conclusions

A 3D lithologic model constructed from 210 boreholes, an interpreted-facies model, and a resistivity model of the subsurface, provide a view that can be used to reconstruct the geologic history of the Cenozoic basin fill in the Amargosa Desert basin. The presence of a thick package of fine-grained sediments at depth, suggest the basin was once closed. These fine-grained deposits are typical of playa and (or) palustrine environments and can be observed at the surface, at the south end of the basin in Ash Meadows. These deposits are interbedded, at depth, with freshwater limestone, and volcanic rocks sourced from both the north and south. Although faults were not explicitly included as part of the 3D modeling, they are well-expressed in the general lithologic patterns in the resulting models. These faulting events probably contributed to the opening of the basin and the ultimate change in the character of the sediment filling the basin. Base level change resulting from the major drainages exiting the basin scoured the fine-grained deposits and exposed rapidly eroding badland topography in the southern Amargosa Desert basin. Coarser sands and gravels typical of alluvial systems were deposited. At the surface, all the surrounding mountain ranges are flanked by prograding alluvial fans. At depth, these fans grade from coarse- to fine-grained sands and gravels as they intersect the basin.

Acknowledgments

Constructive reviews of the draft by Joe Fenelon of the U.S. Geological Survey (USGS) and Harvey Thorleifson of the University of Minnesota greatly improved the quality of the report. Jeremy Havens of the USGS helped to add internal consistency to the illustrations. Funding for this study was provided in part from the USGS National Cooperative Geologic Mapping Program. Additional funding was provided by the Bureau of Land Management, the National Park Service, and the U.S. Forest Service through cooperative agreements with the USGS.

References Cited

Belcher, W.R., Bedinger, M.S., Back, J.T., and Sweetkind, D.S., 2009, Interbasin flow in the Great Basin with special reference to the southern Funeral Mountains and the source of Furnace Creek springs, Death Valley, California, U.S.: Journal of Hydrology, v. 369, no. 1–2, p. 30–43.

Bentley, C.B., Robison, J.H., and Spengler, R.W., 1983, Geohydrologic data for test well USW H-5, Yucca Mountain area, Nye County, Nevada: U.S. Geological Survey Open-File Report 83–853, 34 p.

Blakely, R.J., Hillhouse, J.W., and Morin, R.L., 2005, Ground-magnetic studies of the Amargosa Desert region, California and Nevada: U.S. Geological Survey Open-File Report 2005–1132, 23 p., *http://pubs.usgs.gov/of/2005/1132/*.

Blakely, R.J., Jachens, R.C., Calzia, J.P., and Langenheim, V.E., 1999, Cenozoic basins of the Death Valley extended terrane as reflected in regional-scale gravity anomalies, *in* Wright, L.A., and Troxel, B.W., eds., Cenozoic basins of the Death Valley region: Geological Society of America Special Paper 333, p. 1–16.

Blakely, R.J., Langenheim, V.E., Ponce, D.A., and Dixon, G.L., 2000, Aeromagnetic survey of the Amargosa Desert, Nevada and California: A tool for understanding near-surface geology and hydrology: U.S. Geological Survey Open-File Report 00–188, 39 p., 2 plates, scale 1:250,000, *http://pubs.usgs.gov/of/2000/of00-188/*.

Blakely, R.J., Morin, R.L., McKee, E.H., Schmidt, K.M., Langenheim, V.E., and Dixon, G.L., 1998, Three-dimensional model of Paleozoic basement beneath Amargosa Desert and Pahrump Valley, California and Nevada: Implications for tectonic evolution and water resources: U.S. Geological Survey Open-File Report 98–496, 29 p.

Blakely, R.J., and Ponce, D.A., 2001, Map showing depth to pre-Cenozoic basement in the Death Valley ground-water model area, Nevada and California: U.S. Geological Survey Miscellaneous Field Studies Map, MF–2381–E, scale 1:250,000, *http://pubs.usgs.gov/mf/2002/mf-2381/*.

Byers, F.M., Jr., and Warren, R.G., 1983, Revised volcanic stratigraphy of drill hole J-13, Fortymile Wash, Nevada, based on petrographic modes and chemistry of phenocrysts: Los Alamos National Laboratory Report LA–9652–MS, 23 p.

Carr, W.J., Grow, J.A., and Keller, S.M., 1995, Lithologic and geophysical logs of drill holes Felderhoff Federal 5–1 and 25–1, Amargosa Desert, Nye County, Nevada: U.S. Geological Survey Open-File Report 95–155, 14 p.

Çemen, Ibrahim, 1999, Tectonostratigraphic relationship between the Cenozoic sedimentary successions of the southern Funeral Mountains, Furnace Creek basin, Eagle Mountain, and the north end of the Resting Spring Range, *in* Slate, J.L., ed., Proceedings of Conference on Status of Geologic Research and Mapping, Death Valley National Park: U.S. Geological Survey Open-File Report 99–0153, p. 56–57, *http://pubs.usgs.gov/of/1999/ofr-99-0153/*.

Çemen, Ibrahim, Wright, L.A., and Prave, A.R., 1999, Stratigraphy and tectonic implications of the latest Oligocene and early Miocene sedimentary succession, southernmost Funeral Mountains, Death Valley region, California, *in* Wright, L.A., and Troxel, B.W., eds., Cenozoic basins of the Death Valley region: Geological Society of America Special Paper 333, p. 65–86.

Craig, R.W., and Johnson, K.A., 1984, Geohydrologic data for test well UE-25p#1, Yucca Mountain area, Nye County, Nevada: U.S. Geological Survey Open-File Report 84–450, 63 p.

Denny, C.S., and Drewes, Harald, 1965, Geology of the Ash Meadows quadrangle, Nevada–California—The history of a desert basin and its bordering highlands: U.S. Geological Survey Bulletin 1181–L, 56 p., 1 plate, scale 1:62,500.

Dudley, W.W., Jr., and Larsen, J.D., 1976, Effect of irrigation pumping on desert pupfish habitats in Ash Meadows, Nye County, Nevada: U.S. Geological Survey Professional Paper 927, 52 p.

Fenelon, J.M., and Moreo, M.T., 2002, Trend analysis of ground-water levels and spring discharge in the Yucca Mountain region, Nevada and California, 1960–2000: U.S. Geological Survey Water-Resources Investigations Report 02–4178, 97 p., *http://pubs.usgs.gov/wri/wrir024178/*.

Fridrich, C.J., 1999, Tectonic evolution of the Crater Flat basin, Yucca Mountain region, Nevada, *in* Wright, L.A., and Troxel, B.W., eds., Cenozoic basins of the Death Valley region: Geological Society of America Special Paper 333, p. 169–195.

Fridrich, C.J., and Thompson, R.A., 2011, Cenozoic tectonic reorganizations of the Death Valley region, southeast California and southwest Nevada: U.S. Geological Survey Professional Paper 1783, 36 p. and 1 plate.

Greenhaus, M.R., and Zablocki, C.J., 1982, A Schlumberger resistivity survey of the Amargosa Desert, southern Nevada: U.S. Geological Survey Open-File Report 82–897, 150 p.

Hay, R.L., Pexton, R.E., Teague, T.T., and Kyser, T.K., 1986, Spring-related carbonate rocks, Mg clays, and associated minerals in Pliocene deposits of the Amargosa Desert, Nevada and California: Geological Society of America Bulletin, v. 97, p. 1488–1503.

Hunt, C.B., Robinson, T.W., Bowles, W.A., and Washburn, A.L., 1966, Hydrologic basin, Death Valley, California: U.S. Geological Survey Professional Paper 494–B, 138 p.

Johnston, R.H., 1968, Exploratory drilling, tracer well construction and testing, and preliminary findings, part 1, *in* U.S. Geological Survey tracer study, Amargosa Desert, Nye County, Nevada: U.S. Geological Survey Open-File Report 68–152, 64 p.

Laczniak, R.J., DeMeo, G.A., Reiner, S.R., Smith, J.L., and Nylund, W.E., 1999, Estimates of ground-water discharge as determined from measurements of evapotranspiration, Ash Meadows area, Nye County, Nevada: U.S. Geological Survey Water-Resources Investigations Report 99–4079, 70 p., *http://pubs.water.usgs.gov/wri/wri994079*.

Lahoud, R.G., Lobmeyer, D.H., and Whitfield, M.S., Jr., 1984, Geohydrology of volcanic tuff penetrated by test well UE-25b#1, Yucca Mountain, Nye County, Nevada: U.S. Geological Survey Water-Resources Investigations Report 84–4253, 44 p.

Langenheim, V.E., 1995, Magnetic and gravity studies of buried volcanic centers in the Amargosa Desert and Crater Flat, southwest Nevada: U.S. Geological Survey Open-File Report 95–564, 37 p.

Maldonado, Florian, and Koether, S.L., 1983, Stratigraphy, structure, and some petrographic features of Tertiary volcanic rocks at the USW G–2 drill hole, Yucca Mountain, Nye County, Nevada: U.S. Geological Survey Open-File Report 83–732, 83 p.

Naff, R.L., 1973, Hydrogeology of the southern part of Amargosa Desert in Nevada: Reno, Nev., University of Nevada at Reno, M.S. thesis, 207 p.

Niemi, N.A., Wernicke, B.P., Brady, R.J., Saleeby, J.B., and Dunne, G.C., 2001, Distribution and provenance of the middle Miocene Eagle Mountain Formation, and implications for regional kinematic analysis of the Basin and Range province: Geological Society of America Bulletin, v. 113, p. 419–442.

Nye County Nuclear Waste Repository Project Office (NWRPO), online database of well data from the Early Warning Drilling Program, *http://www.nyecounty.com/ewdpmain.htm*, last accessed November, 2007.

Oatfield, W.J., and Czarnecki, J.B., 1989, Hydrogeologic inferences from drillers' logs and from gravity and resistivity surveys in the Amargosa Desert, southern Nevada: U.S. Geological Survey Open-File Report 89–234, 29 p.

Oatfield, W.J., and Czarnecki, J.B., 1991, Hydrogeologic inferences from drillers' logs and from gravity and resistivity surveys in the Amargosa Desert, southern Nevada: Journal of Hydrology, v. 124, p. 131–158.

O'Leary, D.W., Mankinen, E.A., Blakely, R.J., Langenheim, V.E., and Ponce, D.A., 2002, Aeromagnetic expression of buried basaltic volcanoes near Yucca Mountain, Nevada: U.S. Geological Survey Open-File Report 02–020, 52 p., *http:// pubs. usgs.gov/of/2002/of02-020/*.

Potter, C.J., Sweetkind, D.S., Dickerson, R.P. and Killgore, M.L., 2002, Hydrostructural maps of the Death Valley regional flow system, Nevada and California: U.S. Geological Survey Miscellaneous Field Studies Map MF–2372, scale 1:350,000, 2 sheets with 12-p. pamphlet, *http://pubs.usgs.gov/mf/2002/mf-2372/*.

Raines, G.L., Sawatzky, D.L., and Connors, K.A., 1996, Great Basin geoscience data base: U.S. Geological Survey Digital Data Series DDS–041, CD-ROM, *http://pubs.er.usgs.gov/publication/ds41*; *http://keck.library.unr.edu/Data/GreatBasinGeoScience/*.

RockWare, 2004, RockWorks2004, user documentation, *http://www.rockware.com/*, last accessed November, 2005.

San Juan, C.A., Belcher, W.R., Laczniak, R.J., and Putnam, H.M., 2004, Chapter C. Hydrologic components for model development, *in* Belcher, W.R., ed., Death Valley regional ground-water flow system, Nevada and California—Hydrogeologic framework and transient ground-water flow model: U.S. Geological Survey Scientific Investigations Report 2004–5205, p. 103–136, *http://pubs.usgs.gov/sir/2004/5205/*.

Sawyer, D.A., Fleck, R.J., Lanphere, M.A., Warren, R.G., Broxton, D.E., and Hudson, M.R., 1994, Episodic caldera volcanism in the Miocene southwestern Nevada volcanic field—Revised stratigraphic framework, $^{40}Ar/^{39}Ar$ geochronology, and implications for magmatism and extension: Geological Society of America Bulletin, v. 106, p. 1,304–1,318.

Senterfit, R.M., Hoover, D.B., and Chornack, M.P., 1982, Resistivity sounding investigation by the Schlumberger method in the Yucca Mountain and Jackass Flats area, Nevada Test Site, Nevada: U.S. Geological Survey Open-File Report 82–1043, 39 p.

Snow, J.K., and Lux, D.R., 1999, Tectono-sequence stratigraphy of Tertiary rocks in the Cottonwood Mountains and northern Death Valley area, California and Nevada, *in* Wright, L.A., and Troxel, B.W., eds., Cenozoic basins of the Death Valley region: Geological Society of America Special Paper 333, p. 17–64.

Spengler, R.W., Byers, F.M., and Dickerson, R.P., 2006, A revised lithostratigraphic framework for the southern Yucca Mountain area, Nye County, Nevada: Proceedings of the 11th International High-Level Radioactive Waste Management Conference (IHLRWM), American Nuclear Society, Le Grange Park, Illinois, p. 425–432, *http://www.ans.org/store/i_700317*, or *http://www.osti.gov/energycitations/servlets/purl/894023-bfojGs/*.

Spengler, R.W., Muller, D.C., and Livermore, R.B., 1979, Preliminary report on the geology and geophysics of drill hole UE25a-1, Yucca Mountain, Nevada Test Site: U.S. Geological Survey Open-File Report 79–1244, 43 p.

State of Nevada, Department of Conservation and Natural Resources, Division of Water Resources, online well log database, http://water.nv.gov/data/welllog/index.cfm, last accessed November, 2004.

Steinkampf, W.C., and Werrell, W.E., 2001, Ground-water flow to Death Valley, as inferred from the chemistry and geohydrology of selected springs in Death Valley National Park, California and Nevada: U.S. Geological Survey Water-Resources Investigations Report 98–4114, 37 p.

Stewart, J.H., 1988, Tectonics of the Walker Lane belt, western Great Basin—Mesozoic and Cenozoic deformation in a zone of shear, *in* Ernst, W.G., ed., Metamorphism and crustal evolution of the western United States (Ruby Volume 7): Englewood Cliffs, N.J., Prentice-Hall, p. 683–713.

Stonestrom, D.A., Prudic, D.E., Laczniak, R.J., Akstin, K.C., Boyd, R.A., and Henkelman, K.K., 2003, Estimates of deep percolation beneath native vegetation, irrigated fields, and the Amargosa-River channel, Amargosa Desert, Nye County, Nevada: U.S. Geological Survey Open-File Report 03–104, 83 p.

Stonestrom, D.A., Prudic, D.E., Walvoord, M.A., Abraham, J.D., Stewart-Deaker, A.E., Glancy, P.A., Constantz, Jim, Laczniak, R.J., and Andraski., B.J., 2007, Focused ground-water recharge in the Amargosa Desert basin, *in* Stonestrom, D.A., Constantz, Jim, Ferre, Ty P.A., and Leake, S.A., eds., Ground-water recharge in the arid and semiarid southwestern United States: U.S. Geological Survey Professional Paper 1703–E, p. 107–136, http://pubs.usgs.gov/pp/pp1703/e/.

Swadley, W C, 1983, Map showing surficial geology of the Lathrop Wells quadrangle, Nye County, Nevada: U.S. Geological Survey Miscellaneous Investigation Series Map I–1361, scale 1:48,000.

Swadley, W C, and Carr, W.J., 1987, Geologic map of the Quaternary and Tertiary deposits of the Big Dune quadrangle, Nye County, Nevada, and Inyo County, California: U.S. Geological Survey Miscellaneous Investigations Map I–1767, scale 1:48,000.

Sweetkind, D.S., Fridrich. C.J., and Taylor, Emily, 2001, Facies analysis of Tertiary basin-filling rocks of the Death Valley regional ground-water system and surrounding areas, Nevada and California: U.S. Geological Survey Open-File Report 01–400, 55 p., *http://pubs.usgs.gov/of/2001/ofr-01-0400/*.

Taylor, E.M., 2010, Characterization of geologic deposits in the vicinity of US Ecology, Amargosa Basin, southern Nevada: U.S. Geological Survey Scientific Investigations Report 2010–5134, 194 p., *http://pubs.usgs.gov/sir/2010/5134/*.

U.S. Geological Survey (USGS), 2001, National Water Information System data available on the World Wide Web (Water Data for the Nation), accessed June 10, 2004, at *http://waterdata.usgs.gov/nwis/*.

Whitfield, M.S., Thordarson, William, and Eshom, E.P., 1984, Geohydrologic and drill-hole data for test well USW H-4, Yucca Mountain, Nye County, Nevada: U.S. Geological Survey Open-File Report 84–449, 39 p.

Winograd, I.J., and Thordarson, William, 1975, Hydrogeologic and hydrochemical framework, south-central Great Basin, Nevada-California, with special reference to the Nevada Test Site: U.S. Geological Survey Professional Paper 712–C, 126 p.

Workman, J.B., Menges, C.M., Page, W.R., Taylor, E.M., Ekren, E.B., Rowley, P.D., Dixon, G.L., Thompson, R.A., and Wright, L.A., 2002, Geologic map of the Death Valley ground-water model area, Nevada and California: U.S. Geological Survey Miscellaneous Field Studies Map MF–2381–A, scale 1:250,000, *http://pubs.usgs.gov/mf/2002/mf-2381/*.

Wright, L.A., 1989, Overview of the role of strike-slip and normal faulting in the Neogene history of the region northeast of Death Valley, California-Nevada, *in* Ellis, M.A., ed., Late Cenozoic evolution of the southern Great Basin: Nevada Bureau of Mines and Geology Open-File Report 89–1, Selected papers from a workshop at University of Nevada, Reno, November 10–13, 1987, p. 1–11.

Wright, L.A., Greene, R.C., Çemen, Ibrahim, Johnson, F.C., and Prave, A.R., 1999, Tectonostratigraphic development of the Miocene-Pliocene Furnace Creek Basin and related features, Death Valley region, California, *in* Wright, L.A., and Troxel, B.W., eds., Cenozoic basins of the Death Valley region: Geological Society of America Special Paper 333, p. 87–114.

Wright, L.A., Thompson, R.A., Troxel, B.W., Pavlis, T.L., DeWitt, E.H., Otton, J.K., Ellis, M.A., Miller, M.G., and Serpa, L.F., 1991, Cenozoic magmatic and tectonic evolution of the east-central Death Valley region, California, *in* Walawender, M.J., and Hanan, B.B., eds., Geological excursions in southern California and Mexico: Geological Society of America, Geological Society of America Annual Meeting Guidebook 1991, p. 93–127.

Appendix 1. Lithologic data from driller's lithologic logs from wells in the Amargosa Desert basin

[Appendix 1 can be downloaded from *http://pubs.usgs.gov/sir2014/5003*]

Data compiled within appendix 1 include well location information and lithologic descriptions from driller's lithologic logs from wells in the Amargosa Desert basin. Subsurface data are derived from boreholes drilled in the Amargosa Desert basin for a variety of reasons, including mineral exploration by U.S. Borax (John Rodgers, U.S. Borax, written commun., 1996) and Bond Gold (William Werrell, National Park Service, written commun., 1989), oil and gas exploration (Carr and others, 1995), agricultural and domestic water wells (Naff, 1973; State of Nevada Division of Water Resources, accessed July 2013, at *http://water.nv.gov/data/welllog/index.cfm*), site characterization associated with the U.S. Department of Energy's Yucca Mountain program (Spengler and others, 1979; Bentley and others, 1983; Byers and Warren, 1983;
Maldonado and Koether, 1983; Craig and Johnson, 1984; Lahoud and others, 1984; Whitfield and others, 1984), the Nye County Early Warning Drilling Program to the south of Yucca Mountain (Wood, 2007; Nye County Nuclear Waste Repository Project Office, accessed July 2013, at *http://www.nyecounty.com/ewdpmain.htm*), and wells drilled as part of site-specific studies including the U.S. Geological Survey (USGS) tracer study (Johnston, 1968), monitoring at the US Ecology waste site (Taylor, 2010), research drilling by the USGS on the east side of the basin along the Gravity fault (Wood, 2007) and by Inyo County, Calif., along the eastern flank of the Funeral Mountains (Wood, 2007), and percolation testing in the Amargosa Desert (Stonestrom and others, 2003). Data from measured stratigraphic sections of surface exposures of Cenozoic sedimentary strata were also compiled (Denny and Drewes, 1965; Hay and others, 1986; Çemen and others, 1999; Niemi and others, 2001). Confidential records for 12 drill holes in Inyo County, Calif., were obtained from the State of California Department of Water Resources. For these wells, the drillers' lithologic descriptions are not reported; only the generalized lithologic class interpreted from the descriptions is tabulated.

Well locations are reported as decimal degrees in geographic coordinates, North American Datum of 1927 (NAD 27), and as northing and easting, in meters, in Universal Transverse Mercator (UTM) projected coordinate system, zone 11, North American Datum of 1927 (NAD 27). Elevation at the well location, in meters, is reported relative to mean sea level, referenced to the National Geodetic Vertical Datum of 1929 (NGVD 29). All subsurface intervals are reported in appendix 1 as measured depth—the depth as measured along the length of the borehole. Depth to the top and bottom of each described lithologic interval is given in feet, as originally recorded at the time of drilling, and in meters.

Data compiled as appendix 1 are presented as a Microsoft Excel file that contains two worksheets (Microsoft Corporation, 2013). The first worksheet labeled "Location" has the following information:

- Well name
- Longitude, in decimal degrees, referenced to North American Datum of 1927 (NAD 27)
- Latitude, in decimal degrees, referenced to North American Datum of 1927 (NAD 27)
- Easting, in meters, in Universal Transverse Mercator (UTM) projected coordinate system, zone 11, referenced to North American Datum of 1927 (NAD 27)
- Northing, in meters, in Universal Transverse Mercator (UTM) projected coordinate system, zone 11, referenced to North American Datum of 1927 (NAD 27)
- Elevation of land surface at the well location, in meters, referenced to the National Geodetic Vertical Datum of 1929 (NGVD 29)
- Total depth (TD) of the well, in meters
- Data source
- Alternate well name
- State of Nevada Division of Water Resources (NV DWR) log number
- U.S. Geological Survey National Water Information System Site Identification (USGS NWIS Site ID)
- In model, an identifier indicating whether or not the well is used in the three-dimensional geologic model

The second worksheet is labeled "Lithology" and has the following information:

- Well name
- Top of interval, in feet and meters
- Base of interval, in feet and meters
- Standardized lithologic unit
- Lithologic description

References Cited

Bentley, C.B., Robison, J.H., and Spengler, R.W., 1983, Geohydrologic data for test well USW H-5, Yucca Mountain area, Nye County, Nevada: U.S. Geological Survey Open-File Report 83–853, 34 p.

Byers, F.M., Jr., and Warren, R.G., 1983, Revised volcanic stratigraphy of drill hole J-13, Fortymile Wash, Nevada, based on petrographic modes and chemistry of phenocrysts: Los Alamos National Laboratory Report LA–9652–MS, 23 p.

Carr, W.J., Grow, J.A., and Keller, S.M., 1995, Lithologic and geophysical logs of drill holes Felderhoff Federal 5–1 and 25–1, Amargosa Desert, Nye County, Nevada: U.S. Geological Survey Open-File Report 95–155, 14 p.

Çemen, Ibrahim, Wright, L.A., and Prave, A.R., 1999, Stratigraphy and tectonic implications of the latest Oligocene and early Miocene sedimentary succession, southernmost Funeral Mountains, Death Valley region, California, *in* Wright, L.A., and Troxel, B.W., eds., Cenozoic basins of the Death Valley region: Geological Society of America Special Paper 333, p. 65–86.

Craig, R.W., and Johnson, K.A., 1984, Geohydrologic data for test well UE-25p#1, Yucca Mountain area, Nye County, Nevada: U.S. Geological Survey Open-File Report 84–450, 63 p.

Denny, C.S., and Drewes, Harald, 1965, Geology of the Ash Meadows quadrangle, Nevada-California—The history of a desert basin and its bordering highlands: U.S. Geological Survey Bulletin 1181–L, 56 p., 1 plate, scale 1:62,500.

Hay, R.L., Pexton, R.E., Teague, T.T., and Kyser, T.K., 1986, Spring-related carbonate rocks, Mg clays, and associated minerals in Pliocene deposits of the Amargosa Desert, Nevada and California: Geological Society of America Bulletin, v. 97, p. 1488–1503.

Johnston, R.H., 1968, Exploratory drilling, tracer well construction and testing, and preliminary findings, part 1, *in* U.S. Geological Survey tracer study, Amargosa Desert, Nye County, Nevada: U.S. Geological Survey Open-File Report 68–152, 64 p.

Lahoud, R.G., Lobmeyer, D.H., and Whitfield, M.S., Jr., 1984, Geohydrology of volcanic tuff penetrated by test well UE-25b#1, Yucca Mountain, Nye County, Nevada: U.S. Geological Survey Water-Resources Investigations Report 84–4253, 44 p.

Maldonado, Florian, and Koether, S.L., 1983, Stratigraphy, structure, and some petrographic features of Tertiary volcanic rocks at the USW G–2 drill hole, Yucca Mountain, Nye County, Nevada: U.S. Geological Survey Open-File Report 83–732, 83 p.

Microsoft Corporation, 2013, Microsoft Excel software: One Microsoft Way, Redmond, WA 98052-6399, *http://www.microsoft.com*.

Naff, R.L., 1973, Hydrogeology of the southern part of Amargosa Desert in Nevada: Reno, Nev., University of Nevada at Reno, M.S. thesis, 207 p.

Niemi, N.A., Wernicke, B.P., Brady, R.J., Saleeby, J.B., and Dunne, G.C., 2001, Distribution and provenance of the middle Miocene Eagle Mountain Formation, and implications for regional kinematic analysis of the Basin and Range province: Geological Society of America Bulletin, v. 113, p. 419–442.

Spengler, R.W., Muller, D.C., and Livermore, R.B., 1979, Preliminary report on the geology and geophysics of drill hole UE25a-1, Yucca Mountain, Nevada Test Site: U.S. Geological Survey Open-File Report 79–1244, 43 p.

Stonestrom, D.A., Prudic, D.E., Laczniak, R.J., Akstin, K.C., Boyd, R.A., and Helkelman, K.K., 2003, Estimates of deep percolation beneath native vegetation, irrigated fields, and the Amargosa-River channel, Amargosa Desert, Nye County, Nevada: U.S. Geological Survey Open-File Report 03–104, 83 p.

Taylor, E.M., 2010, Characterization of geologic deposits in the vicinity of US Ecology, Amargosa Basin, southern Nevada: U.S. Geological Survey Scientific Investigations Report 2010–5134, 194 p., *http://pubs.usgs.gov/sir/2010/5134/*.

Whitfield, M.S., Thordarson, William, and Eshom, E.P., 1984, Geohydrologic and drill-hole data for test well USW H-4, Yucca Mountain, Nye County, Nevada: U.S. Geological Survey Open-File Report 84–449, 39 p.

Wood, D.B., 2007, Digitally available interval-specific rock-sample data compiled from historical records, Nevada Test Site and vicinity, Nye County, Nevada: U.S. Geological Survey Data Series 297, 56 p.

Appendix 2. Location and data from resistivity soundings in the Amargosa Desert basin

[Appendix 2 can be downloaded from *http://pubs.usgs.gov/sir2014/5003*]

Data compiled within appendix 2 include station location information resistivity data from resistivity soundings in the Amargosa Desert basin. Vertical electric resistivity soundings were conducted at 136 locations in the Amargosa Desert (Greenhaus and Zablocki, 1982) and 29 locations in the vicinity of Yucca Mountain (Senterfit and others, 1982) to define basement structure and basin-fill characteristics. In each study, raw resistivity data were processed and fitted with a step-function curve that represented a horizontally layered model that best fit the resistivity soundings. The step-function model results from the vertical electric resistivity soundings from all 29 locations in the vicinity of Yucca Mountain (Senterfit and others, 1982) and 50 selected locations from the northern part of the Amargosa Desert (Greenhaus and Zablocki, 1982) were digitized from the paper records.

Station locations of the resistivity soundings were digitized from the location maps in the source reports by georeferencing them in a geographic information system (GIS). Locations are reported as northing and easting, in meters, in Universal Transverse Mercator (UTM) projected coordinate system, zone 11, North American Datum of 1927 (NAD 27). Elevation at the station location, in meters, is reported relative to mean sea level, referenced to the National Geodetic Vertical Datum of 1929 (NGVD 29).

Data compiled as appendix 2 are presented in a Microsoft Excel file that contains two worksheets (Microsoft Corporation, 2013). The first worksheet labeled “Location” has the following information:

- Station name
- Easting, in meters, in Universal Transverse Mercator (UTM) projected coordinate system, zone 11, referenced to North American Datum of 1927 (NAD 27)
- Northing, in meters, in Universal Transverse Mercator (UTM) projected coordinate system, zone 11, referenced to North American Datum of 1927 (NAD 27)
- Elevation of land surface at the well location, in meters, referenced to the National Geodetic Vertical Datum of 1929 (NGVD 29)
- Data source.

The second worksheet is labeled “Resistivity soundings” and has the following information:

- Station name
- Top of interval, in meters
- Resistivity, in ohm-meters

References Cited

Greenhaus, M.R., and Zablocki, C.J., 1982, A Schlumberger resistivity survey of the Amargosa Desert, southern Nevada: U.S. Geological Survey Open-File Report 82–897, 150 p.

Microsoft Corporation, 2013, Microsoft Excel software: One Microsoft Way, Redmond, WA 98052-6399, *http://www.microsoft.com*.

Senterfit, R.M., Hoover, D.B., and Chornack, M.P., 1982, Resistivity sounding investigation by the Schlumberger method in the Yucca Mountain and Jackass Flats area, Nevada Test Site, Nevada: U.S. Geological Survey Open-File Report 82–1043, 39 p.

For more information concerning this publication, contact:
Center Director, USGS Geosciences and Environmental Change Science Center
Box 25046, Mail Stop 980
Denver, CO 80225
(303) 236-5344

Or visit the Geosciences and Environmental Change Science Center Web site at: *http://gec.cr.usgs.gov/*

ISSN 2328-0328 (online)
http://dx.doi.org/10.3133/sir20145003